Fault Classification in Transmission Lines Utilizing Imaging Time-Series and Convolutional Neural Networks and Adaptive Relay Protection

by

Baraa KHABAZ

THESIS PRESENTED TO ÉCOLE DE TECHNOLOGIE SUPÉRIEURE
IN PARTIAL FULFILLMENT OF A MASTER'S DEGREE
WITH THESIS
M.A.Sc.

MONTREAL, AUGUST 29, 2023

ÉCOLE DE TECHNOLOGIE SUPÉRIEURE
UNIVERSITÉ DU QUÉBEC

BOARD OF EXAMINERS

THIS THESIS HAS BEEN EVALUATED

BY THE FOLLOWING BOARD OF EXAMINERS

Mr. Maarouf Saad, Thesis Supervisor
Department of Electrical Engineering, École de Technologie Supérieure

Mr. Hasan Mehrjerdi, Thesis Co-supervisor
Department of Electrical and Computer Engineering, Royal Military College of Canada

Mr. Tony Wong, Chair, Board of Examiners
Department of Systems Engineering, École de Technologie Supérieure

Mr. Pierre Jean Lagacé, Member of the Jury
Department of Electrical Engineering, École de Technologie Supérieure

THIS THESIS WAS PRESENTED AND DEFENDED

IN THE PRESENCE OF A BOARD OF EXAMINERS AND THE PUBLIC

ON AUGUST 24, 2023

AT ÉCOLE DE TECHNOLOGIE SUPÉRIEURE

FOREWORD

Nowadays, the growing and continuous development in the power system field through the implementation of novel concepts and smart methodologies and the rising of integration of renewable energy sources, highlighted the issues and the concerns of ensuring reliable and stable operation of a power system. As result of this evolution, introduced significant variability and uncertainty into the power system to maintain stability in the presence of these intermittent sources requires advanced control and monitoring systems, advanced methodologies to analyze the abnormality in the power system, as well as flexible and adaptive power system designs that can accommodate these new sources of power assets.

Moreover, power system protection is an essential component to ensure the safety and reliability of the electrical power system. The main function of power system protection is to detect and isolate faults or abnormalities in the power system, such as short circuits or overloads, and to disconnect the faulty component or section of the system to prevent further damage. Therefore, the main power system protection characteristic describes the ability to detect and respond to faults in a timely manner that could be caused by a short circuit, loose connection, or lightning strikes in the transmission lines. Mitigating such faults with consistent and authentic protection system reduces the risk of power outages.

Overall, implementing power system protection requires a comprehensive approach that considers the power system's design, operating conditions, and potential fault scenarios. These systems should be designed to be redundant and have built-in backups to ensure that they continue to operate even in the event of potential failure in primary protection layers. A well-designed and maintained protection system is essential for ensuring the safety, reliability, and efficiency of the electrical power system.

ACKNOWLEDGEMENTS

I would like to express my sincere gratitude to all those who have supported and contributed to the completion of this thesis. First and foremost, I extend my deepest appreciation to my supervisors Prof. Maarouf Saad and Prof. Hasan Mehrjerdi for their guidance, expertise, and continuous support throughout this research journey and give me this precious opportunity to further continue my studies. Their invaluable insights and constructive feedback have greatly shaped the direction and quality of this work.

I am indebted to my family especially my father Dr. Mohamed Saeid Khabbaz, my mother and my sisters. And my friends for their unwavering encouragement, understanding, and patience. Their love and support have been a constant source of motivation throughout this challenging endeavor.

Thank you all for your invaluable contributions and support.

Classification des défauts dans les lignes de transport à l'aide de séries temporelles d'imagerie et de réseaux neuronaux convolutifs, et protection par relais adaptatif

Baraa KHABAZ

RÉSUMÉ

Dans cette étude, nous présentons une modèle de classification des défauts dans les lignes de transport, visant à détecter et à classifier ces défauts tout en maintenant une coordination entre les relais primaires et de secours grâce à l'adaptation des paramètres du relais de manière adaptative.

Nous proposons une méthode pour la sélection des relais primaires et de secours à surintensité directionnelle dans les lignes de transmission, ainsi qu'un modèle mathématique pour coordonner ces relais dans un système électrique maillé. Par ailleurs, nous utilisons un modèle de classification des défauts basé sur l'apprentissage profond, plus précisément un réseau neuronal convolutif (CNN) tel qu'AlexNet, pour déterminer le type de défaut dans les lignes de transport. Afin de se conformer à cette approche, les signaux de tension et de courant sont transformés en images à l'aide de la méthode du champ angulaire Gramian. L'objectif est d'exploiter les capacités des réseaux neuronaux convolutifs pour extraire les caractéristiques temporelles des signaux de séries temporelles, et la classification est réalisée à l'aide de réseaux neuronaux entièrement connectés.

Afin d'assurer un fonctionnement synchronisé des relais primaires et de secours, nous modélisons la coordination entre ces relais comme un problème d'optimisation avec des contraintes et une fonction objective. Cette fonction vise à minimiser le temps total de fonctionnement des relais primaires en utilisant le logiciel GAMS. Nous avons utilisé le système d'essai à 9 bus pour déterminer la coordination optimale des relais en fonction du type de défaut, et les résultats ont été évalués par rapport à la littérature existante.

Mots-clés: Classification des défauts, Optimisation, Réseau de neurones artificiels, Coordination des relais

Fault Classification in Transmission Lines Utilizing Imaging Time-Series and Convolutional Neural Networks and Adaptive Relay Protection

Baraa KHABAZ

ABSTRACT

In this research, a model is presented to fault classification in the transmission lines to detect and classify faults while keeping the coordination between the primary and the backup relays by adaptively changing the relay's parameters accordingly.

Furthermore, this research provides a method to select the directional overcurrent primary and backup relays in the transmission lines, as well as the mathematical model for coordinating these relays in a meshed power system. Additionally, a fault classification model based on deep learning as convolutional neural network to determine the fault type within the transmission lines. To comply with convolutional neural network, the voltages and the currents signals were transformed into images using Gramian Angular Field. The objective is to benefit from convolutional neural networks extract the relative temporal features from time-series signals, with the classification process performed using fully connected neural networks.

Additionally, to ensure the synchronized operation of the primary and backup relay relays, the coordination between these relays are modelled as an optimization problem with constraints and objective function. Where the objective function is to minimize the total primary relay operating time by using GAMS software. The 9-bus test system is employed to determine optimal relay coordination according to the fault type and evaluate the results in comparison to existing literature.

Keywords: Fault Classification, Optimization, Neural Network, Relay Coordination

TABLE OF CONTENTS

Page

LIST OF TABLES

Page

LIST OF FIGURES

Page

LIST OF ABBREVIATIONS

DOCR	Directional Over-Current Relay
GAMS	General Algebraic Modeling System
MINLP	Mixed integer non-linear programming
LSTM	Long-short term memory
RNN	Recurrent Neural Network
MRFO	Manta Ray Foraging Optimization
TLBO	Teaching Learning-Based Optimization
ABC	Artificial Bee Colony
CTO	Class Topper Optimization
IPOPT	Interior Point Optimization
ICA	Imperialistic Competitive Algorithm
GA	Genetic Algorithm
SVM	Suport Vector Machine
CNN	Convolutional Neural Network
CT	Current Transformer
VT	Voltage Transformer
TDS	Time Dial Setting
CTI	Coordination Time Interval
GAF	Gramian Angular Field

GASF	Gramian Angular Summation Field
RMS	Root Mean Square
GPUs	Graphics Processing Units
TP	True Positive
TN	True Negative
FP	False Positive
FN	False Negative
NLP	Non-Linear Programming
PSO	Particle Swarm Optimization
DE	Differential Evolution
HS	Harmony Search
SOA	Seeker Optimization Algorithm
SQP	Sequential Quadratic Programming

LIST OF SYMBOLS AND UNITS OF MEASUREMENTS

t	Relay operating time (s)
I	Measured current (A)
I_p	Pick-up current (A)
A, B	Relay Prefixed parameters
r_i	Radius
t_i	Time stamp (s)
$\sigma(z)_i$	Softmax loss
y_n	True label probability
$\hat{y}_n(x_i)$	Predicted class probability
Hz	Samples per second
$T_{primary}$	Primary relay operating time (s)
T_{backup}	Backup relay operating time (s)
$TDS_{i,max}$	Maximum TDS value for a relay i (s)
$TDS_{i,min}$	Minimum TDS value for a relay i (s)
TDS_i	TDS value for a relay i (s)
$Ip_{i,max}$	Maximum I_p value for a relay i (A)
$Ip_{i,min}$	Minimum I_p value for a relay i (A)
Ip_i	I_p value for a relay i (A)
I_{Lmax}	Maximum load current in the transmission lines (A)
I_{Fmin}	Minimum fault current for a relay

INTRODUCTION

0.1 Motivation

Implementing power system protection involves several steps and considerations to ensure that the protection system is effective, reliable, and compatible with the power system's design and operation.

Fault classification and relay coordination are two critical functions in the operation and protection of power systems. Fault classification refers to the process of identifying and characterizing the type of fault occurred in the power system. By accurately and precisely diagnose the fault type, the appropriate response to the fault, such as opening or closing of circuit breakers, will be decided by power system automation and operator to minimize the damage and ensure the safe and reliable operation of the power system.

Moreover, relay coordination is the process of controlling the operation of the protective relays to ensure that the relays will operate appropriately when a fault in the power system occurs. This involves selecting the correct trip settings for each relay, configuring the relays to detect the correct type of fault, and arranging the relays in a sequence in the most effective response to clear a fault.

The protection settings, such as current settings, time delays, must be considered and coordinated according to the fault type, to ensure that the protective devices operate correctly and reliably under normal and fault conditions with providing the necessary redundancy.

0.2 Problem Statement

The problem to be addressed through this study is the need for a protection system that can dynamically adjust the relay's settings and operation to enhance their response to the fault

conditions. This need arises from the necessity to align with the current demands of power protection systems, especially considering the limitations of conventional relays with fixed settings.

0.3 Thesis Statement

In this thesis, the goal is to develop an adaptive protection scheme, that utilizes time-series imaging as features extraction, convolutional neural networks as decision layers, and optimization algorithms to enhance the operation of power system protection.

Moreover, a time-series imaging method will be employed to extract features from temporal measurement data for both voltages and currents, in order to classify faults in transmission lines. To enhance the accuracy of this process, a proposed approach will use a convolutional neural network as feature extraction to the generated images, fully connected neural network, and Softmax layer to make decisions.

After the fault type has been identified, it will enhance the selectivity of the relay's setting. The GAMS software GAMS (2023) will calculate the relay's parameters for achieving optimal relay coordination, while taking into account the fault type, objective function, and constraints. This approach will improve the reliability and efficiency of the power system protection in the electrical grid. The effectiveness of this method will be evaluated by comparing its performance with that of traditional protection schemes.

0.4 Thesis Objectives

The objective behind this research is to develop adaptive protection scheme to mitigate the protection problems. The objectives of this research can be summarized as:

- To briefly summarize the existing literature, this review aims to identify a research gap that has not been adequately addressed in previous studies.

- Identify and analyze the directional overcurrent relays in the protection scheme to select the primary and backup relays.
- Develop a protection scheme that uses the time-series imaging and neural networks to classify the faults in the transmission lines and optimize the relay coordination based on the specific fault conditions.
- Compare the results and evaluate the optimization performance of the proposed scheme with different optimization methods and techniques.
- Identify the limitations and challenges of the proposed scheme and provide suggestions for future improvements.

0.5 Methodology

The main focus of research solution is to enhance the accuracy of fault classification in the transmission system and coordinate between the primary and backup relays while maintain the minimum overall operating time for protection layers.

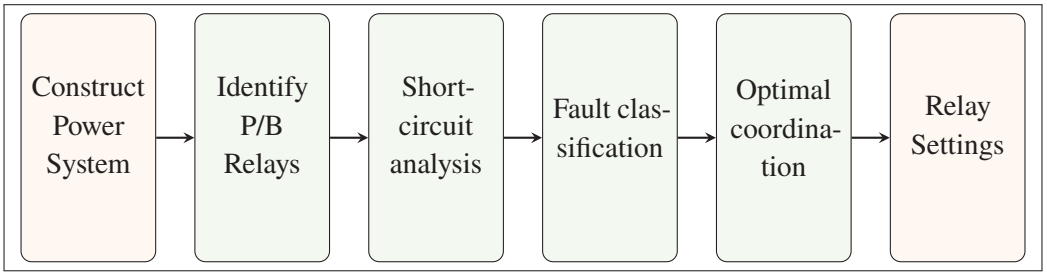

Figure 0.1 Stages for proposed protection scheme

Figure 0.1 shows the proposed approach which consists of multiple stages. The first stage is to identify the layout and the components of the power system. Then, the next stage of this research is to select and identify the primary and the backup relays using LINKNET method, further discussion will be provided in the following Chapter 2.

After calculating the short-circuit analysis and organizing the data, the next step is to apply time-series imaging and convolutional neural networks for feature extraction to classify different types of faults that may occur, such as symmetrical and asymmetrical faults, with a high level of accuracy, as it will be discussed in Chapter 3.

Once the faults have been classified, the fault type has the key role to obtain the optimal operating time for both the primary and backup directional overcurrent relays. In Chapter 4, will find the optimal the coordination between inverse-time directional overcurrent relays according to design constraints and the objective function by selecting the optimal relay settings: pickup currents and time delay settings.

0.6 Thesis Outline

This thesis is organized as follows:
Chapter 1 presents a comprehensive review of existing adaptive protection techniques, algorithms employed for optimal relay coordination, and the implementation of different machine learning techniques for fault classification.

Chapter 2 provides an overview of the principles of protective relays and the approach used to identify primary and backup relays with a case study. Additionally, a brief overview of inverse-time and directional overcurrent relays.

Chapter 3 provides an overview on types of faults in transmission lines, as well as presents the proposed of a fault classifier based on image transformation and CNN as features extractions, whereas utilizes the fully connected neural networks as last stage of classification.

Chapter 4 applies the methods discussed earlier for identifying relay pairs and fault classification and the formulation of the optimization problem to obtain the relay coordination. The 9-bus test system is used for this purpose.

CHAPTER 1

LITERATURE REVIEW

This chapter presents a comprehensive review of the current adaptive protection techniques and solutions used in power system protection. It includes an interpretation of the algorithms used for relay coordination in power system protection. Additionally, the chapter reviews the implementation of various machine learning techniques used for fault classification.

This chapter is structured in two main sections, Section 1.1 related to the adaptive protection techniques and Section 1.2 for machine learning techniques for fault classification.

1.1 Adaptive Protection Schemes

To improve the resilience of power system protection and increase redundancy within the system, it was necessary to develop new adaptive protection schemes. These schemes adapt and utilize a range of methods and approaches to overcome challenges and improve their integrity.

The literature on adaptive protection schemes covers various approaches, such as numerical optimization, fuzzy approaches, and other hybrid methods. Researchers aimed to deploy the developed methods by studying the limitations of previous methods, future implications, and other factors that may impact the reliability of protection systems as shown in Figure 1.1.

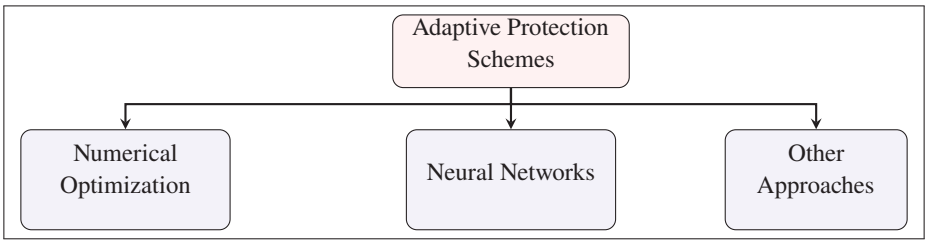

Figure 1.1 Approaches for adaptive protection schemes

El-Hamrawy *et al.* (2022) modeled an adaptive relay scheme by enabling communication paths between all the protection's components and using the GA for optimal relays settings. The proposed scheme recommended to use decentralized networks between the protective

relays to offer fast-acting and exchange the fault status to trip the other relays by overriding the predetermined coordination scheme. However, the deployment of such network must be accompanied with conservative regulations to prevent compromising the overall coordination scheme.

A proposed adaptive protection system has been designed to meet the requirements of IEEE 929 standards in Fani *et al.* (2018). The standard restricted the output current from the solar panels and disconnect them from the grid in case of abnormal conditions. However, this standard could have undesirable impacts on the stability of the grid and on the coordination in the protection system. This is due to the possibility of inducing voltage fluctuation when more solar panels are disconnected. Thus, the occurrence of false tripping caused by relays and results miscoordination in power system protection. The authors proposed to have a group of presets relay's setting for different voltage profiles with the ability to readjust the relay's setting as needed.

By solving bidirectional current problems in modern distribution systems, Ates *et al.* (2016) aligned their model to adapt to modern distribution systems with DG regulations, to build a dynamic framework that monitors DG operating conditions, to produce different actions and control protection mechanisms in the presence of DG units as shown Figure 1.2.

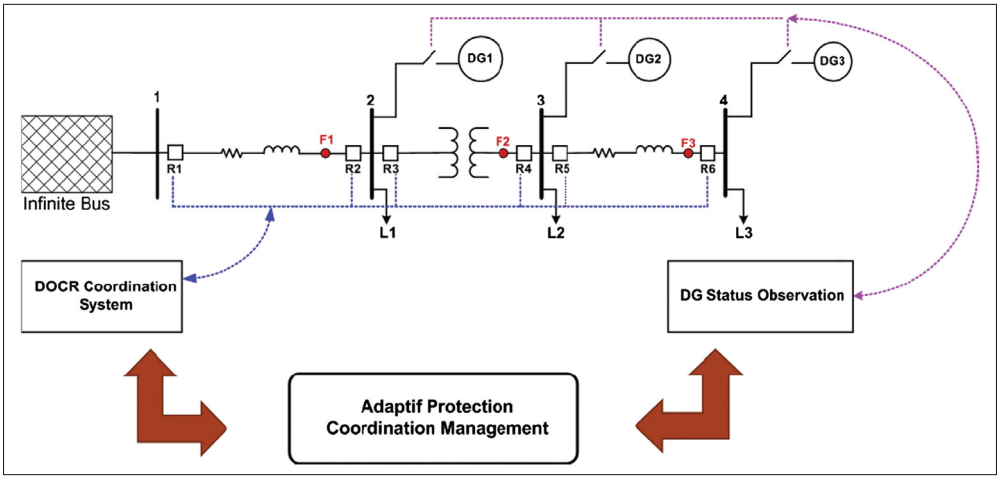

Figure 1.2 Adaptive protection scheme
Taken from Ates *et al.* (2016)

1.1.1 Numerical Optimization for Optimal Relays Settings

Optimal relay coordination in power systems protection refers as the process of selecting the operating characteristics of the protective relays and coordinating the primary and backup relays.Thus, ensure the reliability and resiliency of the protection systems to instantly detect and classify the faults, isolating any faulted sections, restoring the power, and each relay operates appropriately in the event of a fault.

This process typically involves of using of mathematical algorithms to determine the optimal relay's settings and with correct configurations. This literature is exploring the employed algorithm to accomplish this goal.

In Akdag & Yeroglu (2021), the authors suggested to utilize Manta Ray Foraging Optimization algorithm (MRFO) to determine the optimal coordination of Directional Over-Current Relay(DOCR). The MRFO algorithm is based on mimic a biology nature inspired by the foraging behavior of manta rays. That search for the optimal solution in the problem space, where the rays move randomly in the solution space and adapt their search behavior based on the quality of the solutions they found. The authors proposed three different operation modes of protection scheme for distribution system in presence of DGs: all DGs are connected, partial DGs are connected to the grid, and when the distribution system is in island mode.

A new algorithm Teaching Learning-Based Optimization (TLBO) is proposed by Singh *et al.* (2013). The TLBO algorithm is based on the teacher's manner in the class, by motivating the students and extracting the maximum performance. Thereby, the students will be encouraged to elevate their study performance. The objective function of this article is to minimize the coordination time interval between the relays, additionally, to minimize the operating time between backup and primary relays.

Different algorithm is proposed by Uthitsunthorn *et al.* (2011) to obtain the optimal relay setting in distribution systems with the presence of DG. The Artificial Bee Colony (ABC) is based on the behavior of bees, by dividing colony of artificial bees into groups: employed bees, which

they search for the food source with nectar, the highest amount of nectar choose as optimal solution; onlookers, save the location of the food sources; scouts, search for their food sources randomly apart from employed bees.

In context of obtaining the optimal relay coordination, a stochastic optimization technique was applied by Acharya & Das (2022), to overcome the problems associated with complicated optimization that involves local optima and early convergence. The Class Topper Optimization (CTO) inspired by the learning the behavior of students. The CTO algorithm divides the class into sections, each section has a student that continuously improving his/her performance. Each section has topper that represents a local optima; hence, the global solution is the best topper in the class.

A real-time analysis based protection scheme is discussed by Alam (2019). This approach requires acquiring the essential input data such as voltage, current, and status of circuit breakers and determines the optimum setting for the relays. To retrieve the input and control the protective assets, generation, and loads, the IEC 61850 communication protocol is used to adequate the major modification. This scheme alternates and controls the relay's setting rapidly to avoid miscoordination. The Interior Point OPTimization (IPOPT) method is used with an objective function to minimize the operating times of primary and backup relays.

Additional nature-inspired algorithm was addressed by Alaee & Amraee (2021). The Imperialistic Competitive Algorithm (ICA), is based on the concept of imperialism and colonization between the countries in the world. The established imperialist power is identified by the power of the colonies. Hence, the most powerful empire, compared to other empires, is considered the optimal solution.

Particle Swarm Optimization (PSO) is a metaheuristic optimization algorithm inspired by the social behavior of bird flocking. Zeineldin *et al.* (2006) employed PSO to obtain optimal directional relay settings. The PSO concept is to search for the optimal solution within a feasible region. Creating swarm of particles that moves in the feasible region, each particle represents a candidate solution moving in the search-space and update their position and velocity, accordingly.

The best solution found by any particle in the swarm was encountered as the optimal solution. Besides, performing interior point method in prior to initialize the particles within the feasible region; to tolerate the possibility of a single particle being outside the feasible region and to locate the feasible region in coordination model.

Razavi *et al.* (2008) used Genetic Algorithm (GA) to coordinate the overcurrent relays. The basic concept of a genetic algorithm is to simulate the process of natural selection by creating a population of potential solutions to a problem. Then, repeatedly applying a set of genetic operators, such as mutation and crossover, to evolve the population towards better solutions.

Table 1.1 Summary of protection schemes using numerical optimization

Reference	**Methodology**	**Objective**	**Drawback**
Akdag & Yeroglu (2021)	Manta Ray Foraging Optimization	Construct different modes of operations for the relay's setting	Consider only single fault type
Singh *et al.* (2013)	Teaching Learning-Based Optimization	Minimize the total operating time of the protection relays	Not considering adaptive protection scheme nor other fault type
Uthitsunthorn *et al.* (2011)	Artificial Bees Colony Algorithm	Minimize the total operating time of the relays	Not covering the directional feature of the overcurrent relays
Acharya & Das (2022)	Class Topper Optimization	Search for the global solution for the relay coordination	Consider only one relay's characteristics
Alam (2019)	The Interior Point Optimization	Changeable relay's setting via communication protocol	Not conducting fault classification to sufficient protection scheme
Alaee & Amraee (2021)	Imperialistic Competitive Algorithm	Achieve the minimum operation time of the primary relays	Not considering adaptive protection scheme
Zeineldin *et al.* (2006)	Modified Particle Swarm Optimization	To obtain the optimal directional relay setting	Initialization of feasible region does not guarantee the global solution as this process vary to the used algorithm
Razavi *et al.* (2008)	Genetic Algorithm	Coordinate overcurrent relays	Missing adaptive protection scheme

Table 1.1 summarizes the potential benefits and the limitation for the proposed methods in the literature for obtaining the optimal relay setting using for numerical optimization.

1.1.2 Fuzzy Approaches

The fuzzy approach is a mathematical framework to handle the uncertainty and imprecision in data analysis and decision-making. Fuzzy logic is a type of multi-valued logic that allows for intermediate values between true and false.

Swathika *et al.* (2017) presented an adaptive protection scheme for protecting microgrid. A central protection scheme is developed by integrating both fuzzy logic and graph theory. When the fault is detected and its location is identified by the fuzzy logic, the graph theory assists the scheme to isolate only the necessary and the smallest possible portion in the network for clearing the fault. Meanwhile, this scheme cannot be implemented in the meshed power system because of the branching property of the graph method.

A new protection system that combines an Adaptive Fuzzy Inference Model (AFIM) and a heuristic algorithm has been presented by Kumar & Srinivasan (2018). The suggested approach is applying a novel hybrid numerical relay, that permits implementation of real-time adjustment to the relay's setting. The AFIM is used to determine the appropriate relay's current setting. While the heuristic algorithm calculates the time dial settings and reduces the total operating time of the numerical relay.

Momesso *et al.* (2019) presents an adaptable protection system that employs Fuzzy Logic to adjust the pick-up currents setting in the overcurrent relay. Utilizing the Alternative Transients Program - Electromagnetic Transients Program (ATP-EMTP) brings the advantage of enhancing adaptability to the system, by accommodating the modified relay's curves. The outcome of this method led to a reduction of modifying the relay's setting according to the network's topology.

1.1.3 Alternative Approaches

This subsection interprets various methods for adaptive protection schemes, which could include a combination of different approaches or a structured method.

Vasconcelos *et al.* (2022) presents a distribution system with penetration of DGs. The authors suggested combination of methods to have better response and incorporated automated controls for protection system. By utilizing fuzzy logic to have the authority of controlling and changing the protective relays' setting during various operational modes, while utilizing genetic algorithm to optimize and acquire the optimal configuration values for the protective relays.

Coffele *et al.* (2015) focused their solution to develop and implement a four-layers architecture. Figure 1.3 illustrates the proposed approach. The bottom layer of hierarchical model is the physical equipment. The next layer is local control units such as intelligent electronic devices (IDEs) to executes the general commands from the upper layer. The coordination layer is the main layer to accomplish the coordination between the overcurrent relays, compute the power system parameters, and assign new relays setting to the IDEs. In the top of hierarchy is the management layer that regulates, monitors, and supervises the overall performance of adaptive scheme. Different communication protocols were applied between the layers. This method emphasis on calculating the coordination between the relays on real-time basis without considering the fault type.

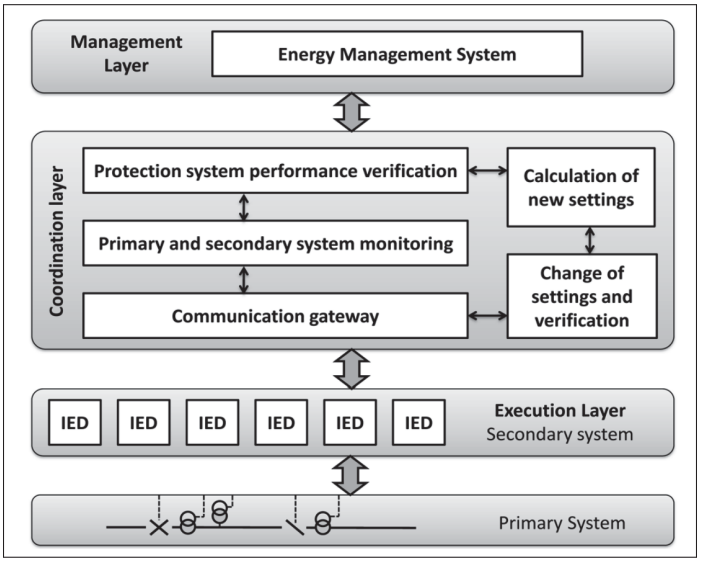

Figure 1.3 Adaptive protection architecture
Taken from Coffele *et al.* (2015)

In their paper, Faria *et al.* (2020), employed a multi-objective optimization technique to determine the optimal location, size, and coordination of protective assets that relied on a probabilistic short-circuit current analysis. Designing a protection scheme that is optimized by the probability of short-circuit occurrence and its location.

Another approach is proposed in Papaspiliotopoulos *et al.* (2017). The suggested approach involves utilizing the hardware-in-the-loop (HIL) simulation method to determine the optimal relay settings. The primary goal is to reduce the total operating time of both the primary and backup systems, and develop a set of configurations to accommodate all possible scenarios. This method used closed-loop procedure along with hardware devices such as RTDS, digital relay and PLC as centralized controllers, and communication infrastructure. One of the key benefits of employing HIL is the ability to detect any defects or failures before implementing the solution.

However, Sharaf *et al.* (2015) believed that the traditional protection strategy, taking pick-up current and time multiplier setting is not sufficient to coordinate the digital relays. Consequently, they introduced new modification to the optimization's variables by assigning two constant related to the relay's characteristics as a variable. As a result, creating non-standard relay's curves that reduces the response time to the fault events by approximately 45% in comparison to two variable conventional coordination schemes.

1.2 Fault Classification using Machine Learning Models

These widely recognized techniques and models in machine learning for data classification. To gain a better understanding and their utilization in the domain of fault classification, these methods are divided into two distinct types.

1.2.1 Generic Machine Learning Methods

These approaches are based on input data that is labeled with corresponding target values. An algorithm learns to predict the output values based on input data that is labeled with corresponding target values. The algorithm is trained on a labeled dataset, where each input data

is associated with its corresponding output value. Selecting an appropriate algorithm or model for classification tasks depends on the nature of the data, computational resources, accuracy, and generalization of the output model.

1.2.1.1 Support Vector Machine Approach

Support Vector Machine (SVM) is a supervised learning algorithm that can be used for classification tasks. Originating from probability hypothesis, Noble (2006), expressed the basic concept SVM model as to find a hyperplane that maximally separates different classes of data points. In the context of power systems, SVM could be utilized to classify different types of faults that may occur in the transmission lines.

Wang & Zhao (2009) applied SVM to transmission line fault classification. The proposed solution is composed of multi-class SVM using a polynomial kernel. To determine the fault location and type, the authors used voltages and currents from a simulated transmission line connected between a source and a load. Thereby, establishing better performance and more accurate results in contrast with Multilayer Perceptions (MLP).

To enhance the response of protective relaying in power transmission systems, a real-time fault classification using SVM model to the protection system is introduced by Youssef (2009). Unlike selecting voltages and currents, the author selected the current phase angles as input data to the SVM model, to reduce the computational resources and gaining higher accuracy.

A multi-class SVM model is investigated by Malathi & Marimuthu (2008) for a system that consists of two generators connected via transmission line. The proposed SVM model has 5 different classes: Single-Line to ground, Line-Line, Double-Line to ground and Three-Phase fault. To classify the dataset, the Radial Basis Function (RBF) kernel was utilized.

Ramesh Babu & Jagan Mohan (2017) follow different directions of applying multiple stages for preprocessing the input data. By implementing Empirical Mode Decomposition (EMD), Intrinsic Mode Functions (IMF) and Hilbert Huang Transform (HHT), respectively, to extract

the features from voltages signals. Hence, the overall efficiency of the classification model under 3 different tuning SVM parameters is 95.33%.

Accomplishing high accuracy of 99.21% to classify 10 fault classes, Ray & Mishra (2016) developed a SVM model for multi-class and the SVM parameters were optimized using PSO. The proposed model uses wavelet transformation to extract and normalize features from fault currents. The system under testing consisted of two voltage sources connected by a 300 km transmission line with a rating of 400kV.

1.2.1.2 Random Forest Approach

Random Forest is a popular ensemble learning algorithm used in machine learning for both classification and regression tasks. According to the research by Breiman (2001), the random forest concept involves the creation of a forest consisting of decision trees. This is achieved by randomly selecting a subset of features and data points at each node of the decision tree. The tree provides a systematic and organized method for analyzing faults, reducing the possibility of missing critical information and increasing the accuracy of fault diagnosis. Which recursively partitions the data into subsets based on the most informative features.

Fonseca *et al.* (2022) classifies the transmission lines fault using a random forest model. Despite that, the SVM reached an accuracy of 99.21%, and the remarkable results from neural networks, the random forest needs less computation time. Regardless of inadequate performance of the random forest model, the authors utilize it with Fourier transform and notch filter for the input data with 10 different fault classes, to achieve reasonable mean accuracy.

Moreover, the penetration of DG raised the issues of the reliability of the power system. Chakraborty *et al.* (2019) implements the random forest model to IEEE 14-bus distribution system with penetration of DGs. The random forest model was specifically developed to accommodate four distinct fault classes.

1.2.2 Neural Networks Methods

Machine learning and artificial intelligence can be used in fault classification in the power system domain in a variety of ways. For example, supervised learning algorithms can be trained on historical data to classify different types of faults, such as short circuits and line faults. Unsupervised learning algorithms can be used to identify patterns in the data that may indicate the presence of a fault.

1.2.2.1 Feed-forward Neural Network

The feedforward neural network is a type of artificial neural network where information flows only in one direction as shown in Figure 1.4. The input data is fed through input layer to a series of interconnected hidden layers, to reach the output layer to have the final verdict, without feedback nor loops to update the weights of neural networks.

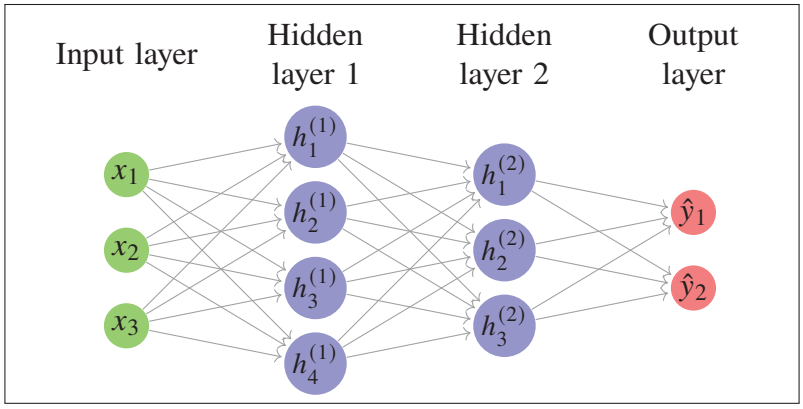

Figure 1.4 Simple feed-forward neural network
Taken from Svozil *et al.* (1997)

This concept was carried out by Elnozahy *et al.* (2019) for fault classification and location. Using normalized fault voltages and currents from the simulation, this method astonishing accomplished an accuracy of 100%; however, the neural model cannot represent a factual experiment to develop a more complex power system, due to a relatively simple system: a generator connected to the load via transmission lines.

1.2.2.2 Backpropagation Neural Network

In contrast to the feed-forward neural networks, the backpropagation approach is based on updating the neuron's weighted sum incrementally until the network's output is sufficiently close to the desired output, which allows the error to be propagated backward through the network by computing the error with respect to the true output.

Jamil *et al.* (2015) followed this approach for fault classification in their predetermined power system. The input data for the neural networks are voltages and currents. To ascertain the neural network that is most effective, versatile and accurate, a comprehensive evaluation was conducted, which included testing different numbers of layers.

Adopting this approach to be implemented in microgrid concept, Yu *et al.* (2019) conducted backpropagation neural network for microgrid protection faults detection and classification. The suggested approach achieves an accuracy level of 97.6%, surpassing the accuracy levels of random forest and SVM, which are 94% and 93.3%, respectively, in terms of classification. Additionally, the model exhibits exceptional performance even when there is noise present, with results that nearly to 97.55%.

1.2.2.3 Convolutional Neural Network

Convolutional Neural Networks (CNNs) are a type of deep learning algorithm that is particularly compatible for image classification tasks. The CNNs are composed of multiple layers of artificial neurons, each of which is designed to learn a specific feature from the input data. The layers are organized in a hierarchical manner, similar to the suggested architecture by Lecun *et al.* (1998) in Figure 1.5 to represents AlexNet architecture. According to O'Shea & Nash (2015), the CNN can be segmented into three fundamental components that comprise its basic functionality:

In Gu *et al.* (2018), the Convolutional Neural Network (CNN) is a type of artificial neural network that specifically designed for image classification. The input image is passed through a series of convolutional layers that apply a set of filters.

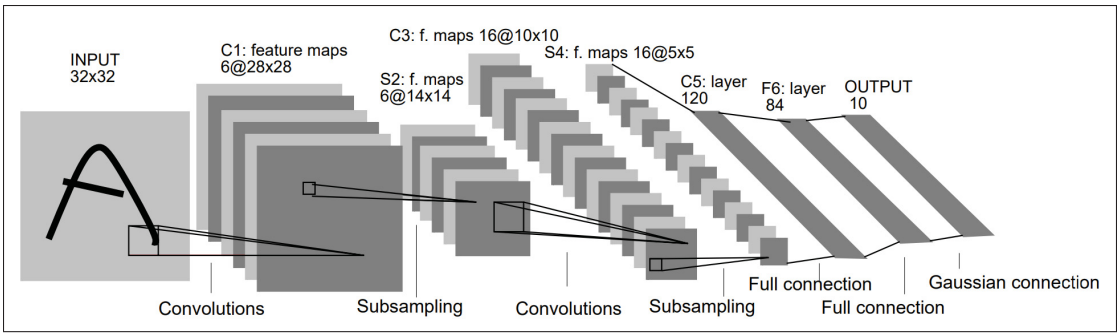

Figure 1.5 CNN for AlexNet architecture
Taken from Lecun *et al.* (1998)

The filters perform a mathematical operation called convolution, which involves sliding a window over the input image and computes the dot product of the window at each group pixels. This process results in a set of feature maps, each representing a different aspect of the input image. Moreover, this approach was modified by Sánchez-Reolid *et al.* (2022), to perform one-dimensional convolutional process for ECGs signals.

Furthermore, Mitra *et al.* (2022) adopted the same approach for CNN classification, by gathering the three-phase fault currents over a predetermined cycle and combined them into one flatten vector as represented in Figure 1.6. Eventually, the fully connected neural layers receives the output from the convolutional layers as one flatten vector, which perform classification task based on the extracted features.

Integrating DGs into distribution systems raises concerns regarding of fault classification and detection. Rai *et al.* (2021) demonstrated the implementation of a CNN approach that doesn't require feature extraction, instead using directly the voltages and currents signals captured by the power system sensors.

In an alternative method of applying CNN, Tong *et al.* (2021) formulated a novel approach using CNN model and graph theory. By incorporating adaptable changes to the topology of the power system network during transient fault conditions.

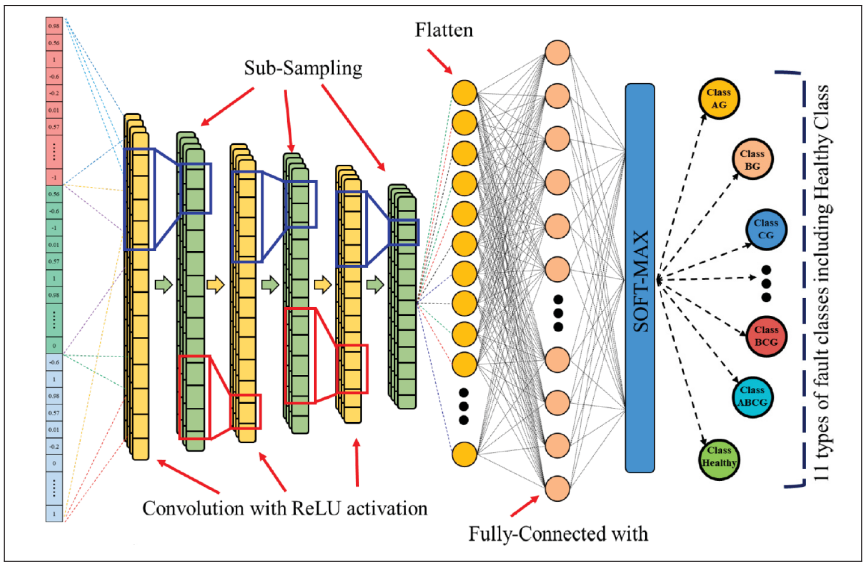

Figure 1.6 Combined features CNN
Taken from Mitra *et al.* (2022)

This approach incorporates prior topology information into the neural network. This results in an effective scheme for fault detection and a more generalized model.

An LSTM is a type of recurrent neural networks architecture to handle the vanishing gradient, whereas the gradients can become insignificant as they propagate through time. The LSTM introduces a memory cell and three gates to increase effective and the ability to handle time-series data and capture long-term dependencies. Zhang *et al.* (2018) suggested a combination of LSTM and SVM techniques for identifying and categorizing fault within China southern power grid. Whereas the LSTM will predict the occurrence the fault by capturing the temporal features for the system characteristics such as current, voltage, and active power; the SVM model will classify the fault according to trained model.

1.3 Research Gap within the Existing Literature

There is a shortage of research in the area of adaptive protective schemes that cover fault classification and the appropriate setting of directional overcurrent relays based on the type of fault, as well as adjusting relay settings based on the specific fault type as shown in Table 1.1.

Table 1.2 Summary of machine learning methods for fault classification

Reference	Approach	Signal Type	Overall Accuracy	Pre-processing phase	Noise Tolerant
Wang & Zhao (2009)	SVM	Voltages & currents angels & magnitude	Error = 0.07	Normalized	No
Youssef (2009)	SVM	Currents phase angles	Not discussed	Wavelet transformation	No
Malathi & Marimuthu (2008)	SVM	Currents	98.8%	Wavelet transformation	No
Ramesh Babu & Jagan Mohan (2017)	SVM	Voltages	95.33%	EMD & IMF & HHT	No
Ray & Mishra (2016)	SVM & PSO	Voltages	99.21%	Wavelet & Normalization	No
Fonseca *et al.* (2022)	Random forest	Voltages	91.49%	Fourier transformer and notch filter	No
Chakraborty *et al.* (2019)	Random forest	Voltages	81%	Random sampling	No
Elnozahy *et al.* (2019)	Feed-forward NN	Voltages & currents	100%	Normalization	No
Jamil *et al.* (2015)	Back propagation NN	Currents	Correlation: 0.93788	Normalization	No
Ngaopitakkul & Bunjongjit (2013)	Back propagation NN	Currents	97.22%	Wavelet transformation	No
Yu *et al.* (2019)	Back propagation NN	Current magnitudes	97.55%	Discrete Wavelet transformation	Yes
Mitra *et al.* (2022)	CNN	Currents	99.75%	Combined three-phase currents	Yes
Rai *et al.* (2021)	CNN	Voltages & currents	99.97%	No	No
Tong *et al.* (2021)	CNN	Voltages magnitudes	98.28%	Rearrange topology by graph theory	Yes
Zhang *et al.* (2018)	LSTM + SVM	Voltages & currents & active power	97%	Normalization	No

Additionally, there is a lack of papers that provide optimal relay settings for different types of faults.

Table 1.2 shows the previous studies on fault classification using machine learning involved variety of using of conventional methods like SVM and random forest, as well as neural networks models such as backpropagation NN, CNN and LSTM. By utilizing both types of algorithms, researchers have made progress to classify faults using variation of system's characteristics and noise. The objective of improving fault classification accuracy with removing noise was not successfully met. Instead, the approach employed in this study involved utilizing time-series imaging to extract relevant features, which were then used to train a CNN model. This method was selected to leverage the advantages of CNNs in image classification.

The objective of this research is to fulfill the research gap in adaptive protection schemes by creating a novel adaptive protection scheme that is specifically designed to modify relay settings according to the type of fault encountered. This will enable a more accurate response to faults without sacrificing the coordination or sensitivity of the protection equipment, the aim is to establish a protection scheme that is exceedingly robust and resilient.

In the upcoming chapters, this work will provide a detailed discussion of the proposed approach and the mathematical representation of achieving the best possible coordination among relays and accurately identifying faults.

CHAPTER 2

POWER SYSTEM PROTECTION

2.1 Introduction

This chapter presents an overview of protective relay principle and the approach used to identifying the primary and backup relays. Additionally, outlines the mathematical model of relay coordination in a meshed power system, focusing on coordinating the primary and backup relays. Also, a brief overview for inverse-time and directional overcurrent relays.

This chapter is organized as follows Section 2.2 represents an overview of power system protection along with function of directional overcurrent relays. Section 2.3 describes the approach for identifying the primary and backup relays and a case study. The coordination between the primary and backup relays is demonstrated in Section 2.4. A conclusion is provided in Section 2.5.

2.2 Protective Relay Principle

Protective relaying is a branch of power protection that deals with the protection of electrical power system from unpredicted faults. A protective relay is an electrical device that automatically detects faults in an electrical system and operates a circuit breaker to isolate the faulty portion of the system to prevent damage or power flow irruption throughout the power systems.

The fundamental concept of protective relaying is to identify any irregularities or abnormal conditions in the electrical power system, such as transmission line faults. The protection system has to be adequate to quickly detect the faults and efficiently response to fault conditions to minimize damage to the power system.

Power system protection is a crucial component of an electrical power system. The main components of power system protection, as shown in Figure 2.1, are:

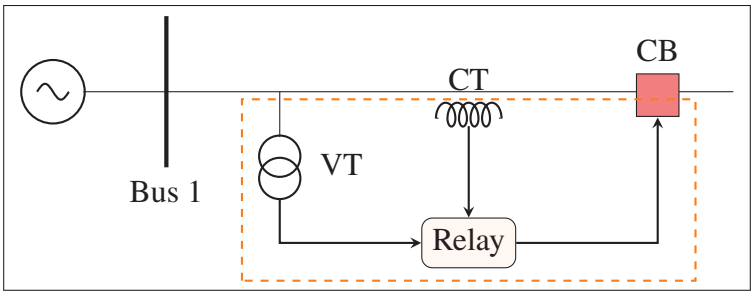

Figure 2.1 Protection system principle

- **Sensing devices:** These are the devices that detect power system parameters. They include current transformers (CT) to monitor the current, voltage transformers (VT) to monitor the voltage, and directional elements. These devices provide the input signals to the protective relays.
- **Control devices:** These are the electronic devices that receive input signals from the sensing devices and make decisions to isolate faults in the power system. They include overcurrent relays, distance relays, and differential overcurrent relays.
- **Circuit breakers:** These are the mechanical switches that physically isolate faults in the power system. They are usually operated by the protective relays.

These main components work concurrently to provide the required protection with integrity and reliable power system protection scheme, guaranteeing the secure and dependable operation of the power system. Additionally, in modern power system protection, as mentioned by Leelaruji & Vanfretti (2012), communication devices are integrated to enable communication channels between the relays, different network assets, and control systems. This integration enables the implementation of digital relay protection using multiple communication protocols.

2.3 Identifying the Primary and Backup Relays

In this section, a comprehensive overview is provided of the operational principles of the Directional Over-Current Relay (DOCR). Besides, describes the approach to select the backup relay or set of backup relays to a specific primary relay in power systems.

2.3.1 Directional Over-Current Relays

The directional over-current relay is a type of protection relays that is based on two parameters the current direction and the current magnitude. Glover *et al.* (2012) defined Inequality 2.1, a relay operates within the specified angle difference, which is represented by $\phi - \phi_1$, where ϕ_1 is a variable that determines the desired direction and ϕ is the angle difference between the current and the reference voltage. When current flow within this range, the relay identifies this as a fault condition and open the associated circuit breaker.

$$-180^\circ < (\phi - \phi_1) < 0^\circ \tag{2.1}$$

However, the current is considered as normal operation, when the current flow outside the defined range. Figure 2.2 illustrates a 4-bus power system that utilizes DOCR. For example, when the fault occurred in transmission line 3, the fault current will flow towards the least impedance. Which in this case the current will flow from bus 3 and bus 4 towards to the fault point.

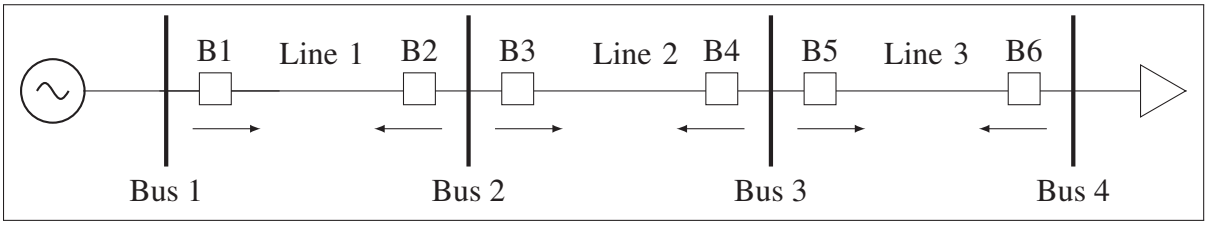

Figure 2.2 4-bus system

To clear the fault, the pair relays (B5, B6) are considered the primary DOCR relays to respond and disconnect line 3 from the power source and the load. However, if the fault is not cleared by the primary relay (B5) due to any inoperative circumstances, the subsequent backup relays to respond to (B5) will be a sequence of relays according to their proximity to the fault, with (B3) being the closest to respond and isolate the fault and (B1) being the farthest to the latest to respond the fault.

However, to avoid overlapping between the primary and backup relays, an introduction to have a time delay between the relays is elaborated in Section 2.4.

Although identifying the DOCR relay pairs of protection in the previous simple 4-bus system is relatively straightforward using graph theory in Al-Roomi (2022), larger and more complex systems require more effective and complex algorithms to identify these pairs. The next subsection 2.3.2 represents the LINKNET method to identify the primary and the backup relays.

2.3.2 LINKNET Method

Warford (2002) presented the linked-list as a linear data structure used for data storage and organization. The list consists of a sequence of elements called nodes, each node has two parameters value and pointer. The value stores the data whereas the pointer refers to the next node in the list to link all the nodes. However, the last node in the list typically has a pointer to a null, indicating the end of the list.

The LINKNET is type of linked-list structure that was utilized by Laway & Gupta (1994) to identify the primary and backup relays. This structure has the advantage of changing the list according to power network topology by to adjust the list size based on the number of buses in the power system.

This linked-list consists of three main vectors: List, Next, and Far. Constructing the vectors is based on power network topology, such number of the buses and the location of the buses.

- **List**: is a vector that has all the buses for given system and the vector's size equal to total number of the buses. Each value in this vector represents the DOCR that direction points towards that bus.
- **Next**: this vector stores the all DOCRs that are related to a specific bus and the pointer refer to the next DOCR.
- **Far**: unlike List vector, this vector has the DOCR that is located close to a bus and the DOCR direction points away from that bus.

The flowchart in Figure 2.3 provides the detailed steps of Birla *et al.* (2004) implantation of LINKNET method. Firstly, the List vector is constructed by recording all the buses with corresponding DOCRs in this vector by scanning all the branches. The branch is defined as a transmission line that connects two different buses along with their corresponding relays. Then, the Next vector is constructed from List vector containing all the DOCRs whose directions are directed towards.

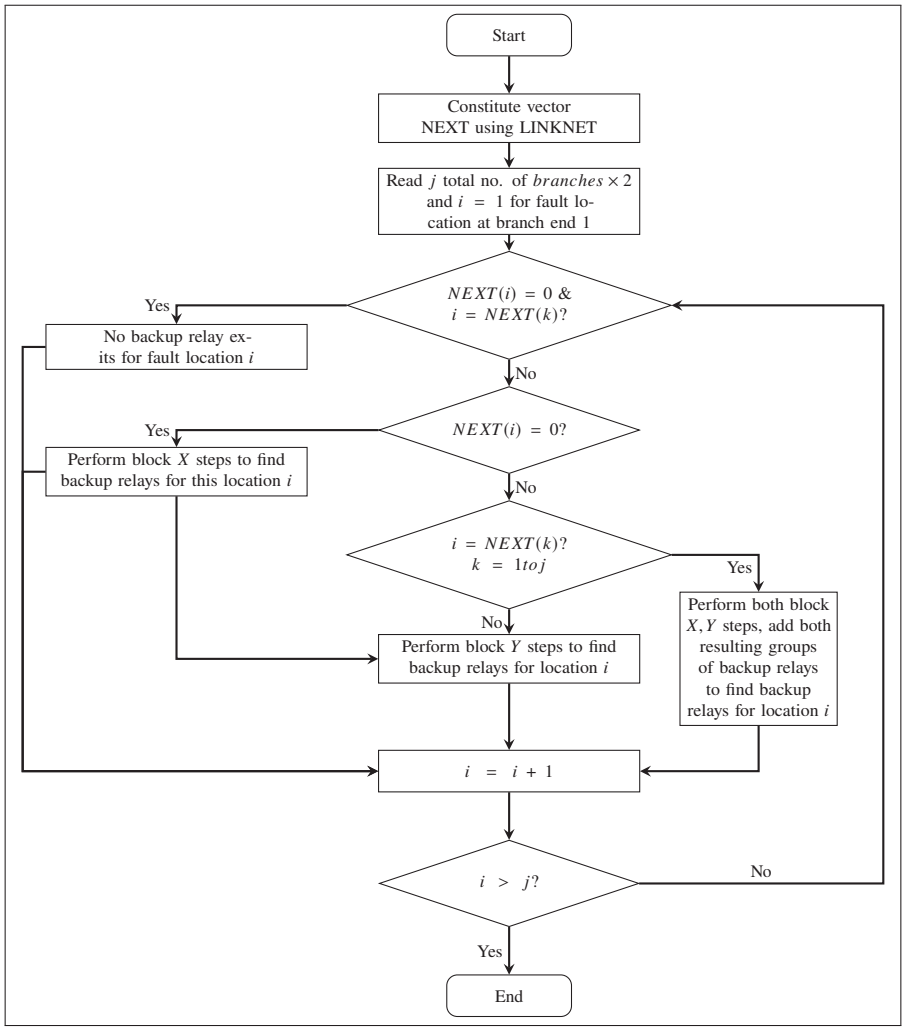

Figure 2.3 LINKNET flowchart
Taken from Birla *et al.* (2004)

Subsequently, the Next vector has different scenarios according to its values. For example, when the Next vector has pointed to zero value and position k, then, it indicates that is no backup relays.

However, when Next vector has pointed to zero value in specific direction such as clockwise around a bus, thus, continue searching in counterclockwise until find all the backup relays.

Then, proceed to the next value in the List vector, the flowcharts block X and block Y ("see Appendix I, Figure-A I-1a,b") respectively, assets the main flowchart in Figure 2.3 to obtain the backup relays. This process should be repeated until all available backup relays associated with a particular bus are acquired and the Next vector reaches a zero pointer. Finally, the Far vector assists in determining relay pairs by identifying the inverse of Far vector which corresponds to the far-bus faults that are associated with the respective primary relay.

2.3.3 Case Study: 5-Bus System

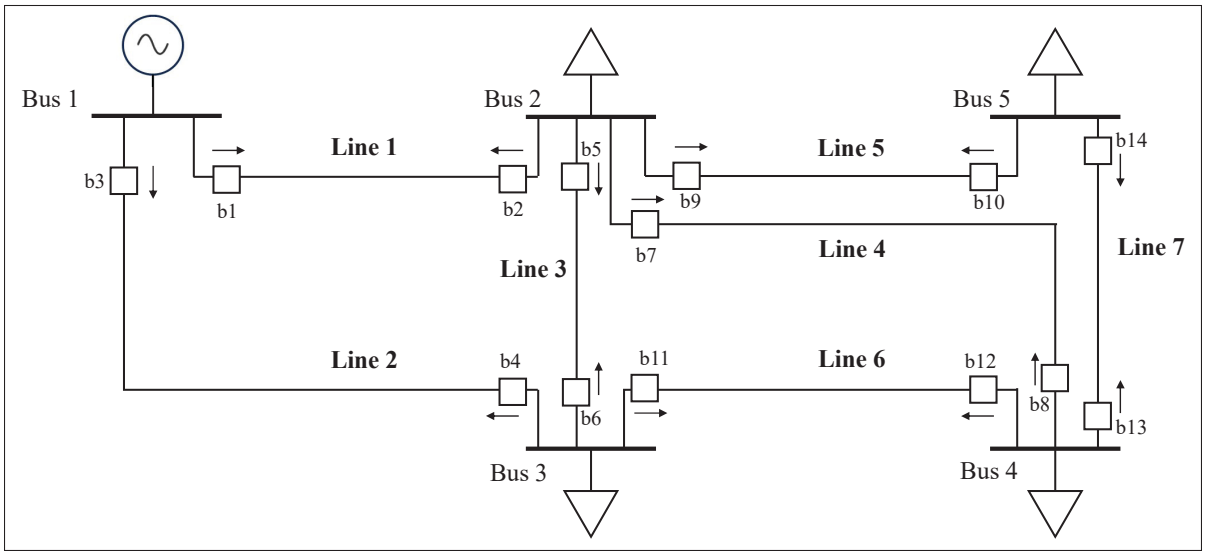

Figure 2.4 5-bus system with directional overcurrent relays

Figure 2.4 illustrates a 5-bus system with directional overcurrent relays installed near to each bus. This system consists of a power source connected to bus 1 and four loads distributed from bus 2 to bus 5. All the buses are connected via seven transmission lines creating seven different branches. In this system, a 14 DOCRs are installed in the transmission lines, where each relay has an ongoing direction from its nearby bus, as depicted in Figure 2.4. The numbering of DOCRs depends on the labeling of the transmission lines, starts from bus 1 to bus 2, then, bus 2

to bus 3,4, and 5, respectively. The line 7 connects the bus 4 and 5. This numbering scheme is crucial to determine the relay pairs using LINKNET.

To identify the primary and backup relays pairs for 5-bus system, LINKNET method is constructed and solved using MATLAB. Figure 2.5 illustrates the LINKNET structure for the List and Next vector. The List has two variables (Bus, nearby relays), while the Next vector acts as a pointer. Considering the blue arrows points from List towards Next vector, whereas the red arrows indicate the next backup relay in List.

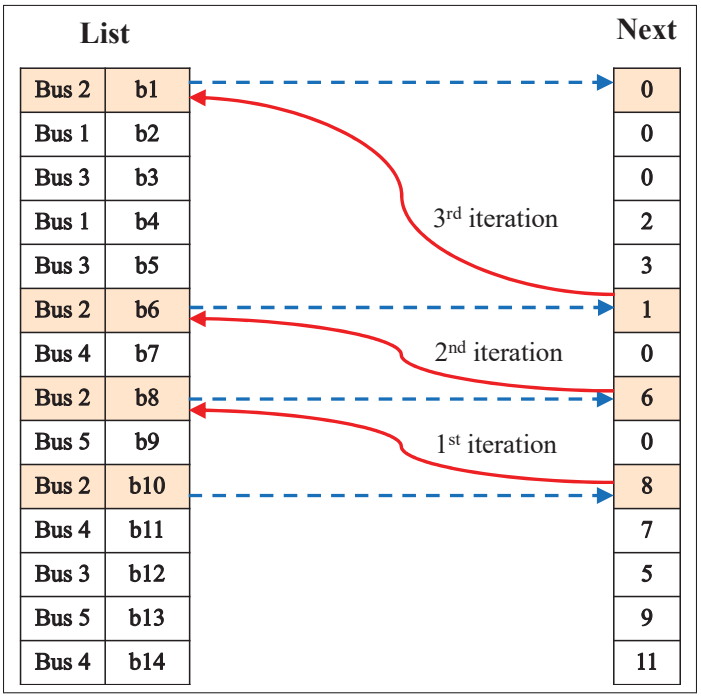

Figure 2.5 Graphical representation of LINKNET for List and Next vectors

To provide an example of selecting backup relays for (b2) relay. Starting with (b10), which is the last element that bus 2 has and it is located as the 10^{th} element in List. Subsequently, this element points to the 10^{th} element in Next vector which has value of 8. Then, track the pointer from Next vector to the 8^{th} element in the List. Hence, the (b10) and (b8) are initial backup relays, nevertheless, this process is required to be iterated until the Next vector reaches zero values. In this case, the process is iterated three times and produced a set of backup relays (b10,

b8, and b6) for the (b1) relay. The detailed LINKNET structure and vectors are presented in ("see Appendix I, Table-A I-1").

The Primary relays can have multiple backup relays. For example, the relay (B2), located at nearby bus 2, is considered as the primary relay and responsible to respond if a fault occurred in line 1. When the fault occurred, the current tends to flow through the path of least impedance. Therefore, it is necessary to interrupt the current flowing towards bus 2. Then, the relays (b6, b8, and b10) are considered as the backup relays for (b2). This set of backup relays is selected because they are directed towards to bus 2. Table 2.1 summarizes all the primary and backup relays for each line.

Table 2.1 Primary and backup pairs relays for 5-bus system

Line	Primary relay	Backup B1	Backup B2	Backup B3
Line 1	1	4	–	–
	2	10	8	6
Line 2	3	2	–	–
	4	12	5	–
Line 3	5	10	8	–
	6	12	3	–
Line 4	7	10	6	–
	8	14	11	–
Line 5	9	8	6	–
	10	13	–	–
Line 6	11	5	3	–
	12	14	7	–
Line 7	13	7	–	–
	14	9	–	–

2.4 Primary and Backup Relays Coordination

This section covers the mathematical representation and an overview of inverse-time directional overcurrent relays. Additionally, after identify the primary and the backup relays in previous Section 2.3, this section demonstrates the process of coordinating relay pairs to ensure their simultaneous operation, which involves introducing a time delay between the relays.

2.4.1 Inverse-time Directional Overcurrent Relay

After specifying the direction of the relays in Section 2.3.1, it becomes essential to integrate time into the DOCR relays. This allows for better control over their operation, ensuring that the backup relays do not trigger simultaneously during a fault event.

Glover *et al.* (2012) presents an inverse-time overcurrent relay to measure the current flowing through a circuit and compares it to a predetermined magnitude set-point. When the fault current exceeds the pickup current, then, the relay energized and trips the corresponding circuit breaker to protect the power system, this called pickup current I_p. Besides, the Time Dial Setting (TDS) is an adjustable parameter in the relay to have a time delay and consequently enabling the adjustment of the relay's operating time.

Furthermore, the operating time of an inverse overcurrent relay is a decisive parameter in determining the effectiveness of the protection scheme. The relay's operating time t, according to Al-Roomi (2022), is the following Equation 2.2:

$$t = TDS \times \frac{A}{(\frac{I}{I_p})^B - 1} \tag{2.2}$$

Where is:

- TDS: is time dial setting,
- I: is the current measured from CT sensor.
- I_p: the pick-up current is the current level at which the relay starts to respond to an overcurrent condition.
- A, B: are prefixed parameters that are depending on the specific application and the desired time-current characteristic of the relay.

The shape and position of the time-current curve are determined by the design of the protective device and the requirements of the system being protected, where A, B determines the slope

and the curvature of the time-current curve and the influence on to relay's response to the fault. According to Al-Roomi (2022), the IEC-60255 standard, the relay's mode of operations are standard inverse, very inverse, extremely inverse, and long-time standby earth fault as Table 2.2:

Table 2.2 Inverse-time parameters

Relay characteristics	**A**	**B**
Standard inverse	0.14	0.02
Very inverse	13.5	1
Extremely inverse	80	2
Long time standby Earth fault	1	120

The inverse-time directional overcurrent relay has some key characteristics such as adjustable settings for the pickup current, time delay, and current direction, these characteristics enable the relay to be adjusted according to the specific requirements of the power system.

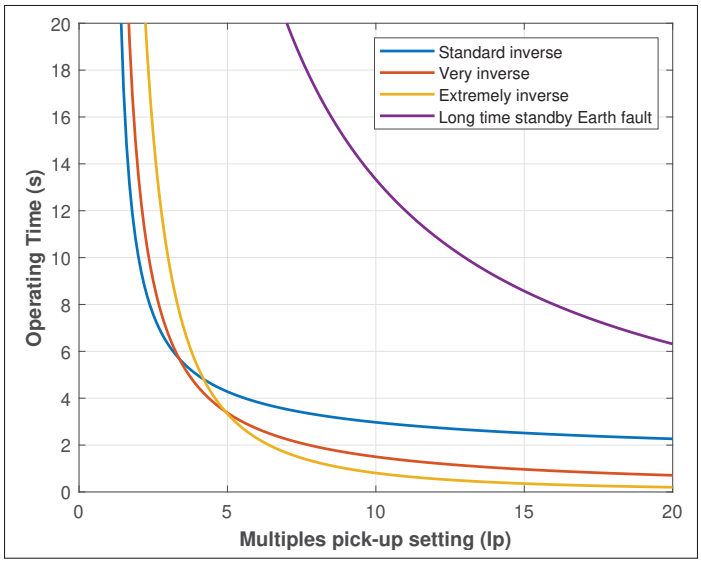

Figure 2.6 Inverse-time overcurrent relay characteristics

The operating time of the relay depends upon the level of fault current. That is, the time of operation of a relay depends on the configuration (I_p, TDS) and the severity of the fault current. Hence, the inverse overcurrent relay's response to overcurrent is inversely proportional to the duration and the magnitude of the current, this relation is plotted as a time-current curve as

shown in Figure 2.6. This graph can determine the total time taken by a relay to respond and rectify a fault. Thereby, the relay can be configured to swiftly respond or in extremely manner.

2.4.2 Definition of Relay Coordination

Coordinating relays in a power system is crucial to guarantee that only the relay closest to a fault operates to isolate the faulted section, while the backup relay operate after a specified time delay, allowing the primary relay sufficient time to respond.

This approach prevents unnecessary tripping and minimizing power flow disruptions for the unaffected areas. Thus, provides an extra layer of protection and adds redundancy to improve the reliability and effectiveness of the protection scheme. This time delay between the primary relay and backup relay is defined as Coordination Time Interval (CTI).

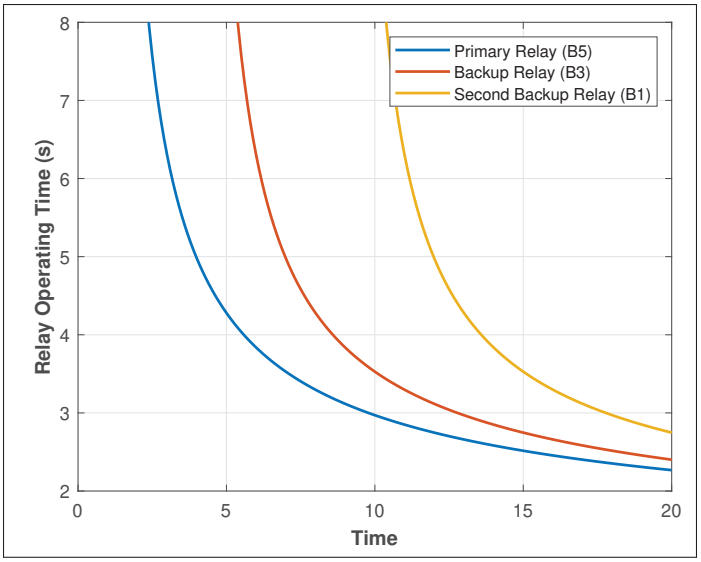

Figure 2.7 Relays operating time in 5-bus

Figure 2.7 shows different operating times for set of relays during the occurrence of a fault in 4-bus in Figure 2.2. It is noticeable that the (b5) relay have the shortest operating time and operate faster response, whereas the (b1) relay requires a longer time to activate.

Consequently, a well-designed protection schemes will have a time-current characteristic that is optimized for the specific application, providing rapid and effective protection against faults while minimizing unnecessary tripping. The optimization for obtaining the relay's parameters is further described in details in subsequent Chapter 4.

2.5 Conclusion

In conclusion, identifying primary and backup relays are important components in the protection scheme of power systems. Whereas the primary relays are considered the main relays to initialize a response to nearby faults occurred in the transmission lines, the backup relays provide a second layer of protection in case the primary relays were failed due to any circumstances. Using LINKNET approach to identify the relay pairs. Together, the List and Next vectors enable efficient execution of identifying the relay pairs for the entire system.

The inverse-time directional overcurrent relays has various parameters, including time, direction, and fault current magnitude to be configured for each relay. Moreover, the CTI represents the time delay between the activation of the primary and backup relays. This parameter is critical to ensure that the primary relay operates first, and the backup relay only intervenes if the primary relay fails to operate within the designated time. The time-current curve is typically based on the specific requirements of the system being protected, taking into account factors such as the expected range of fault currents, the sensitivity of the protection scheme, and the response time needed to minimize damage to the system.

CHAPTER 3

FAULT CLASSIFICATION USING GRAMIAN ANGULAR FIELD AND NEURAL NETWORKS

3.1 Introduction

This chapter proposes the concept of a fault classifier based on image transformation and neural networks. The purpose of this approach is to utilize convolutional neural networks in collaboration with image transmission to extract the features from a given time-series signals and fully connected neural networks are used to perform the classification process.

This chapter provides a comprehensive overview for the transmission lines faults in Section 3.2. Furthermore, the proposed model will be introduced in Section 3.3. Besides, provides a background and mathematical representation for converting time-series into images in Section 3.4 and feature extraction using convolutional layers in Section 3.5. In addition, addressing the issue of overfitting in a classifier in Section 3.6 and proposed neural network architecture in Section 3.7. Lastly, a case study focusing on a particular power system is presented in Section 3.8 and conclusion in Section 3.9.

3.2 General Overview of Transmission Line Faults

The power system is a crucial infrastructure for modern society, and its stable operation is essential for ensuring the continuity of various services. However, power system faults can occur due to various reasons such as equipment failure or natural disasters.

Fault classification is the process of recognizing and categorizing different types of faults in a power system. It is a major part of power system protection, as it is used to differentiate between normal and abnormal conditions and classification the type of fault, the location of the fault, and the duration of the fault. Common types of fault include short-circuit and grounding.

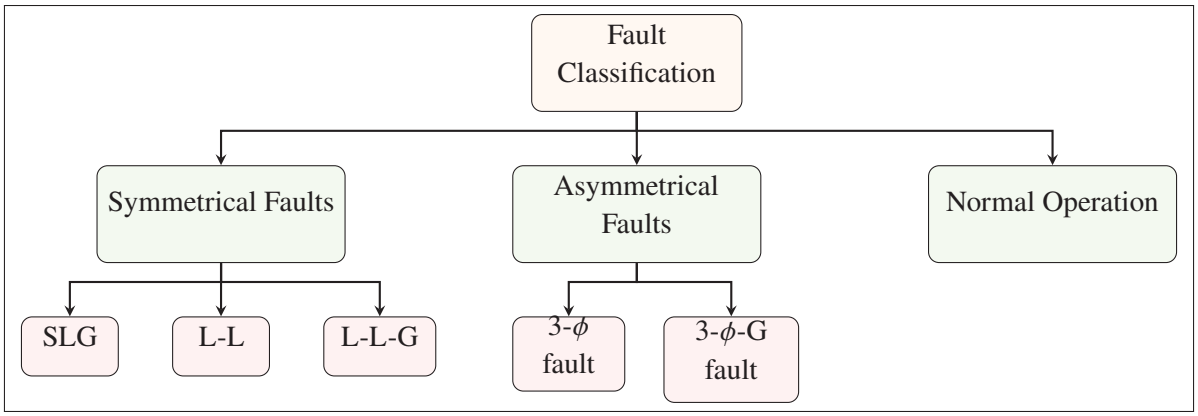

Figure 3.1 Overview for transmission line faults

Figure 3.1 depicts the three primary categories of power system situations, including symmetrical and asymmetrical faults, as well as normal operation.

- **Symmetrical fault** occurs when there is an equal amount of current flowing in all three phases of a three-phase system. Symmetrical faults produce equal current magnitudes in each phase and are usually easier to detect and diagnose compared to asymmetrical faults. For example:
  - **Three-Phase fault:** This fault occurs when all three phases of the line connected simultaneously. This can cause a large amount of current to flow through the system, which can damage equipment and potentially cause a power outage.
  - **Three-Phase-to Ground fault:** alike three-phase fault, this fault is when all the phase are connected to each other and connected to the ground.
- **Asymmetrical fault** occurs when the current flowing in each phase is not equal. Which results more complex faults than symmetrical faults because of in unbalanced currents and voltages situations in the power system. For example:
  - **Single-Line-to-Ground fault:** where single line of the transmission line is affected and contacted with a ground reference point. It can be caused by equipment failure, insulation failure, or loose connections.

- **Line-to-Line fault:** occurs when a short circuit occurs between two transmission lines, where two phases were connected together. Falling a tree branch or other debris across could impose such a fault.
- **Line-to-Line-to-Ground fault:** similar to line-to-line fault, this fault comes when two phases connected conjointly and into contact with the ground.

In any of these scenarios, the power flow in the line will be disrupted potentially causing in lack of power and damage to the transmission line. Additionally, the extent and severity of the damage caused by the fault will depend on factors such as the type of fault, its location, and how long it persists. Hence, it is crucial to design a protection system capable of withstanding all types of faults, detect, and respond to faults in a timely manner.

3.3 Proposed Architecture for Fault Classifier

To fulfill the research's objective, a fault classifier that is based on machine learning is developed. The phases to produce the proposed fault classifier are illustrated in Figure 3.2.

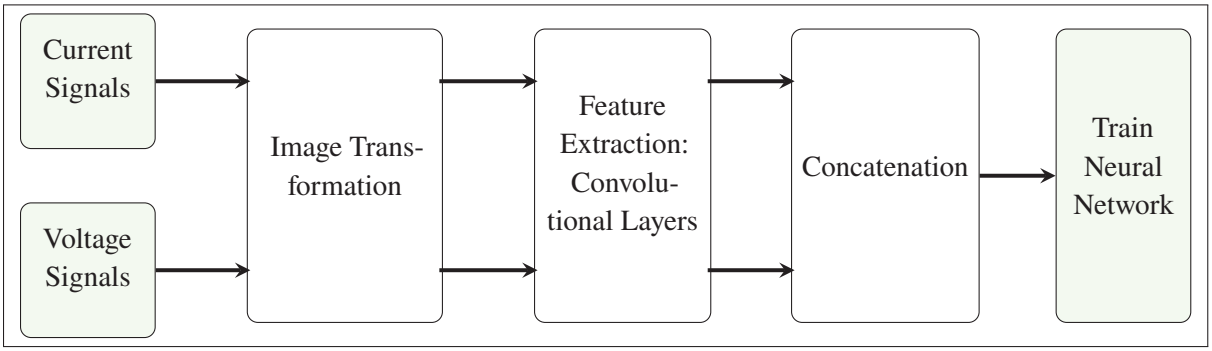

Figure 3.2 Stages for proposed fault classification

The preliminary phase is to collect the raw data from the transmission lines and provide these data as input to the neural network to classify and whether the fault occurred in the transmission lines or not and determine fault type. Since the voltages and the currents are obtained from a power system networks as variation between the amplitudes and time, it is necessary to obtain the data at a predefined sampling rate. In order to ensure the compliance with standards, this research

has been conducted with considering the established standards. As outlined in Bishop & Nair (2023) IEC 61850-9-2, the signals are required to be sampled at 4,800 samples per second (Hz).

Thereafter, the fault signals are visually represented using GAF and each voltage and current phases are transformed as a separate a RBG image. This is accomplished through mapping the time-series data to a 2D matrix, where each element of the matrix represents a pixel of from an image. The details of the transformation are elaborated in Section 3.4.1.

The next phase is to extract the temporal features from the generated images using sequence of convolutional layers, where in this research, the selected architecture for performing the convolutional operations is AlexNet as proposed in Krizhevsky *et al.* (2017). Each generated image from both the voltages and the currents will pass through this architecture creating six vectors of features.

Then, a concatenation layer is applied to produce a single vector that contains all the image's features. Whereas, the last phase is to do the classification task using customized fully connected neural network. Further details and various techniques that were implemented to address the issues associated with deep learning are provided in the subsequent Section 3.6.

3.4 Transforming Time-Series Signal to Images

In this section, a brief overview of transforming time-series to images is presented using Gramian Angular Field with its mathematical expressions.

3.4.1 Gramian Angular Field

Gramian Angular Field (GAF) is an approach that aims to capture the dynamics of the time-series in a visual format as an image. Figure 3.3 represents the essential phases for time-series transformation, as indicated by Wang *et al.* (2015). Starts by normalizing the time-series to mitigate the effect of anomalies and extreme values. The next step is to transform the signals

from Cartesian coordinates, Figure 3.3a, to Polar coordinates, Figure 3.3b, to gain the advantage of preserving its temporal dependency.

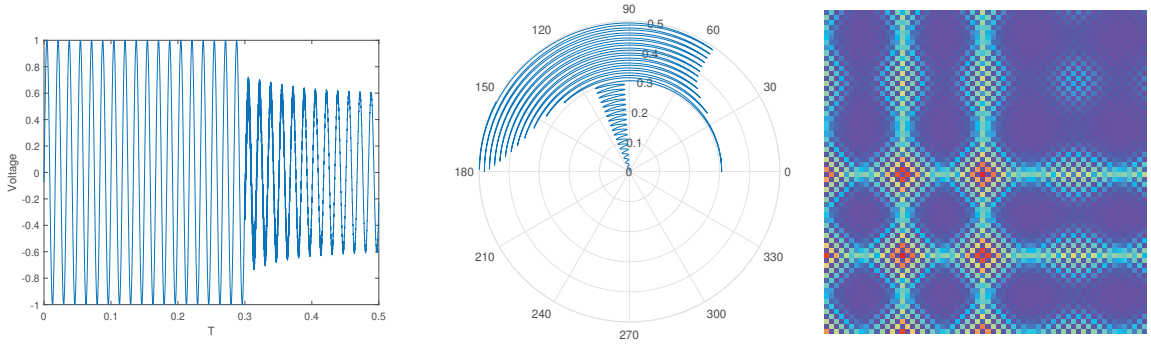

a) Signal in Cartesian coordinate b) Signal in Polar coordinate c) Signal in GASF encoding

Figure 3.3 The conversion of a signal from time-series into GASF image

For a given time-series $X = \{x_1, x_2, \ldots, x_i\}$, where x_i represents value at a given time. Then, Equation 3.1 is used to normalize the signal, where the minimum value in the time-series will be transformed to -1, and the maximum value will be transformed to 1. Hence, the values in the given interval will be scaled proportionally between -1 and 1 .

$$\tilde{x}_i = \frac{(x_i - \max(X)) + (x_i - \min(X))}{\max(X) - \min(X)} \tag{3.1}$$

Expression 3.2 transforms the normalized time-series $\tilde{x}_i$ into an angular representation using the inverse cosine function. The radius r_i is then calculated by dividing the time stamp t_i by a constant factor N to regularize the span of the polar coordinate system.

$$\begin{cases} \phi_n = \arccos(\tilde{x}_i), & -1 \leq \tilde{x}_i \leq 1, \tilde{x}_i \in \tilde{X} \\ r_i = \frac{t_i}{N}, & t_i \in \mathbb{N} \end{cases} \tag{3.2}$$

Consequently, the amplitude changes as the sequence values vary with time and are transformed into angular changes in the polar coordinate system. In Wang *et al.* (2015), a temporal correlation

is established between every pair of points. That is, the cosine summation of their respective angles yields the identified temporal correlation; therefore, it leads to generating the Gramian Angular Summation Field (GASF), as shown in relation 3.3. Hence, each pixel in the image corresponds to the value in the GASF.

$$GASF = \begin{bmatrix} \cos(\phi_1 + \phi_1) & \cos(\phi_1 + \phi_2) & \dots & \cos(\phi_1 + \phi_n) \\ \cos(\phi_2 + \phi_1) & \cos(\phi_2 + \phi_2) & \dots & \cos(\phi_2 + \phi_n) \\ \vdots & \vdots & \ddots & \vdots \\ \cos(\phi_n + \phi_1) & \cos(\phi_n + \phi_2) & \dots & \cos(\phi_n + \phi_n) \end{bmatrix} \tag{3.3}$$

Figure 3.4 shows different generated images. When a transmission line experienced a fault, the generated images will produce visually similar images in Figures 3.4a,b,c. However, Figure 3.4d depicts the signal with normal operation or in case where this phase is not affected by the fault, as will be elaborated in Section 3.8.5.2.

The reconstruction of the GASF matrix from the image format and the subsequent restoration of the original time-series can present a significant challenge due to the uncertainty arising from the randomness as elaborated in Wang *et al.* (2015). This uncertainty is directly influenced by factors such as the resolution of the images, number of pixels, and its mapping in the color spectrum.

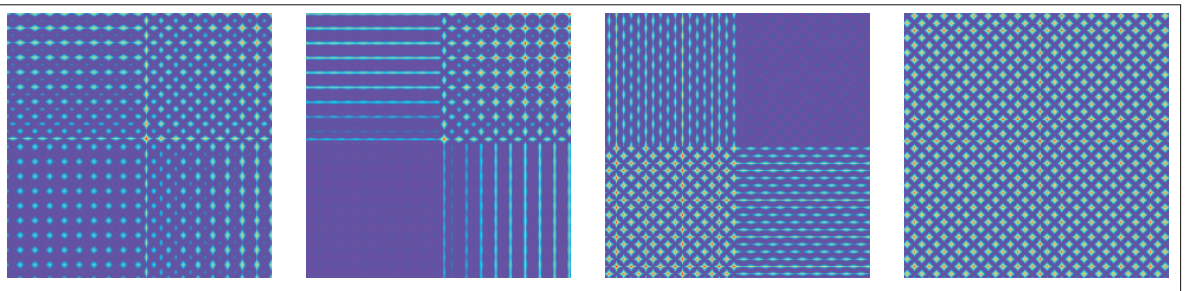

a) Far fault current signal from a bus

b) Near fault current signal from a bus

c) Voltage fault signal

d) No fault signal

Figure 3.4 Comparison between faulty and no-faulty images

3.4.2 Data Acquisition

Choosing an appropriate sampling plays a crucial role in determining the characteristics of the signal and the ability to capture finer details and variations within the sampled signal. Therefore, adjusting the sampling time allows to control the level of detail captured in the GAF matrices. A shorter sampling time means that more data points are available within a given time interval, resulting in a higher resolution GAF matrix, providing a more detailed representation of the essential dynamics. Thus, the images will be affected directly with the desired level of accuracy and the quality of temporal features that will be extracted for classification task.

Choosing an appropriate sampling time depends on the specific application's standard. Consequently, the data are sampled at 4,800 samples per second (Hz), following the established standards of data acquisition in digital substations the IEC 61850-9-2. The number of samples and the duration of the fault which will be addressed in the Section 3.8.

3.4.3 Difference Between Image's Size

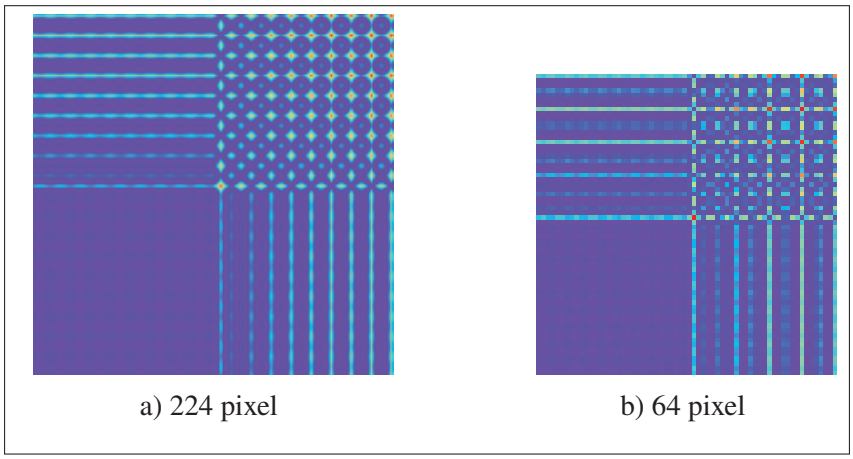

Figure 3.5 Comparison between current signals with different images sizes

Selecting the size of GASF matrix will leads to different image sizes, each with different pixel intensities. Figure 3.5 illustrates the comparison between the image sizes 224px and 64px, respectively. With an increase in GASF dimensions, the number of pixels increases accordingly.

Consequently, this allows for the preservation of more temporal features, affecting the image quality and maintain the details to the original time-series data.

The selection of the GASF matrix size is made while taking into consideration the recommended resolution and ensuring compatibility with commonly used convolutional layers such as AlexNet or VGG-16. These convolutional layers are specifically designed to optimize computational performance and maximize the extraction of essential features. This will be further elaborated in Section 3.5.

3.5 Features Extraction using Convolutional Layers

In this section, a discussion is presented to elaborate the methodology to extract the essential features from the generated images utilizing AlexNet.

3.5.1 Convolutional Layers

The function of these layers is to execute mathematical operations on the input images and further convoluted layers, which enables the extraction of relevant features after each convolutional operation. O'Shea & Nash (2015) defined the convolution operations as performing an element-wise multiplication with the corresponding pixel of an image by sliding a small matrix, referred to as a filter or kernel, over the image. Figure 3.6 shows the multiplication between the numerical values of an image and the kernel, where the sum of that operation generating new layer of features. However, the movement of a kernel over the pixels depends on an architecture's structure. This parameter known as the stride, which dictates whether the window could be fully or partially multiplied with next window of pixels.

Once the convolutional layer is produced, then passed through a nonlinear activation function, such as a ReLU (Rectified Linear Unit) or sigmoid functions, to introduce nonlinearity in the model. This nonlinearity helps to determine whether to activate the associated neuron with its corresponding label by saturating the output.

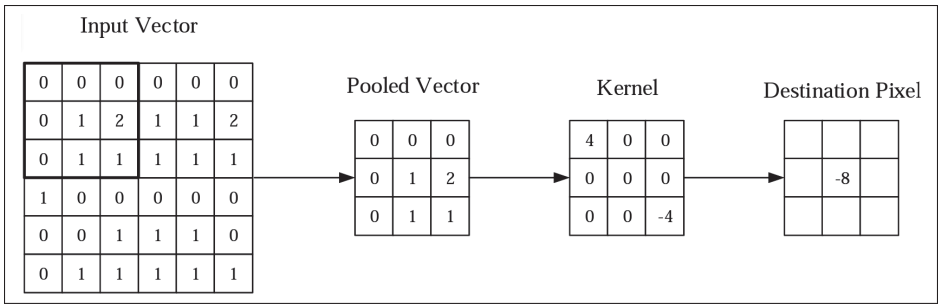

Figure 3.6 CNN operation
Taken from O'Shea & Nash (2015)

3.5.2 Pooling Layers

Albawi *et al.* (2017) outlined these layers as they used to reduce the dimensions the convolutional layers and further filtering the redundant features, thereby reducing the computational resources and time, while extracting more important features and minimizing the number of unnecessary features. This is achieved by dividing the input layer into smaller windows and returns either the max or the average value within each window as depicted in Figure 3.7.

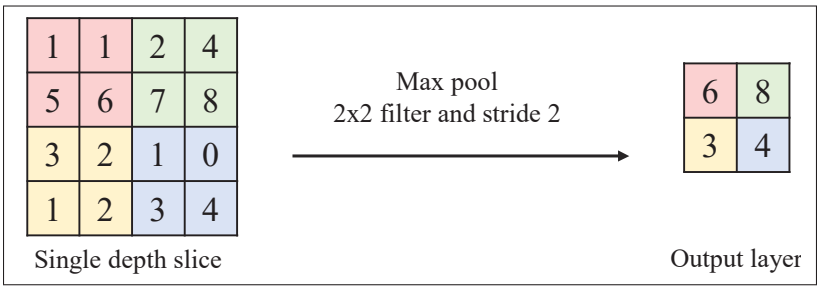

Figure 3.7 Map-pooling operation
Taken from Albawi *et al.* (2017)

3.5.3 AlexNet Architecture

Krizhevsky *et al.* (2017) proposed the architecture of AlexNet that consists of five convolutional layers. The first and the second convolutional layers followed by max-pooling layers, whereas the third, the fourth and the fifth are connected in series without any pooling layers between them.

Table 3.1 summarizes the AlexNet architecture, displaying the details of each layer including its size, kernel, stride, and padding.

In this model, the Rectified Linear Units (ReLU) are utilized as activation functions. Moreover, the authors introduced the concept of using Graphics Processing Units (GPUs) for training the deep neural networks, which significantly accelerated the learning process. Hence, this architecture is selected in this research to extract the temporal features from the images.

Table 3.1 AlexNet architecture, Krizhevsky *et al.* (2017)

Layer	**Size**	**Kernel**	**Stride**	**Padding**
Input layer (image)	$224 \times 224 \times 3$			
Convolution layer 1	11×11	96	4	–
Max pooling	3×3	–	2	–
Convolution layer 2	5×5	256	1	2
Max pooling	3×3	–	2	–
Convolution layer 3	3×3	384	1	1
Convolution layer 4	3×3	384	1	1
Convolution layer 5	3×3	256	1	1
Max pooling	3×3	–	2	–
Output Layer	$256 \times 5 \times 5$			

In the context of fault classification in transmission lines, a total of six measurements are gathered from a bus, which are divided into three from voltage readings and three from current readings, representing the three different phases (A, B, and C).

Figure 3.8 illustrates the process of extracting temporal features from the generated images discussed in the previous Section 3.4. In this process, the AlexNet is utilized to extract these features from each image. As a result, a flatten feature vector of size 6,400 is generated for each image which also indicates for each phase. The output features obtained from this step will be utilized in the subsequent Section 3.7.

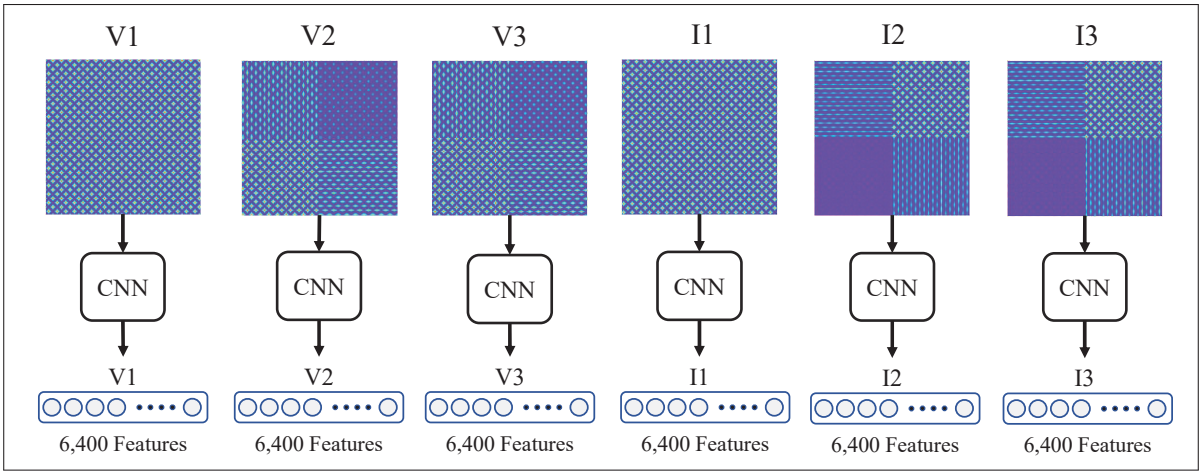

Figure 3.8 Extracting features from images using CNN

3.6 Handling Overfitting in Classifier

In neural networks, the overfitting problem is the main issue when training the neural networks. It occurs when the neural network model becomes more specific and starts to memorise the dataset. Hence, the model loses its ability to provide a general model and its capability to predict the correct class when an external instance is given to the model.

To classify the faults from the transmission lines, the collected voltages and currents will be sampled from the same transmission line, forming the dataset. However, it is important to note that training a classifier with such a dataset, which exhibits similarities, could potentially lead to overfitting issues during the training process. To avoid such an issue during the training, the proposed solutions are discussed as follows:

3.6.1 K-fold Cross-Validation

The concept behind K-fold cross-validation is to provide insights into the trained neural network model in generalization capabilities and to assess the model's performance to accurately classify the dataset. The implementation for this technique is based on dividing the training dataset into

equal K-fold subsets. For each fold, the elements within each subset are selected randomly for both training and validation subsets shown in Figure 3.9.

The model is trained and validated K times. During each training iteration, one of the K folds is selected as the validation set, while the remaining folds are used as the training set.

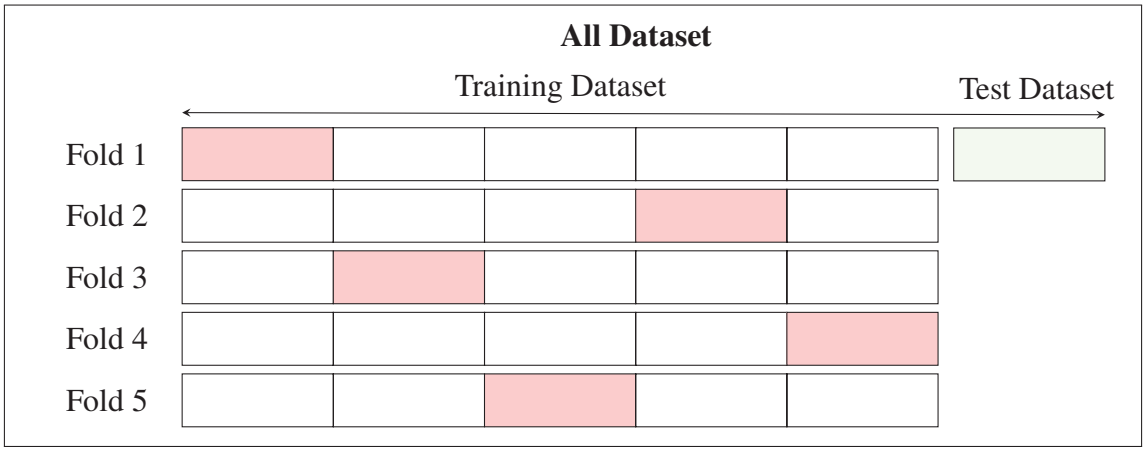

Figure 3.9 K-Fold cross validation

Thus, the validation subset is used as testing subset in each iteration to assess and validate the model's performance. This approach provides more comprehensive evaluation and helps mitigate the variance associated with a single train-test split.

3.6.2 Dropout

Srivastava *et al.* (2014) discussed the concept of introducing the dropout layers between the dense layers in the neural network. The proposed approach is to randomly drop or neglect neurons and backward passes between the layers during each training iteration. As a result, there are different neurons and distinct backward passes after each training iteration are activated, leading to more robust model and resistant to the redundant data and generalizes better to any external data.

3.7 Classification Task

This section provides the proposed neural network architecture with overview about softmax activation function and cross-entropy loss.

3.7.1 Proposed neural network architecture

In this research, a modification is made to AlexNet architecture to accommodate the model's requirements. The produced feature vectors from the convolutional layers from the previous Section 3.5 are concatenated into a single vector. The resulting vector, consisting of features extracted from three-phase voltages and three-phase currents has 38,400 features in 1-dimensional vector as shown in Figure 3.10.

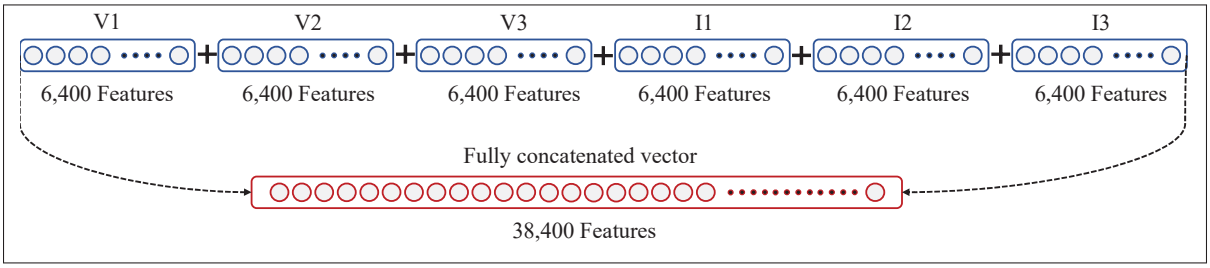

Figure 3.10 Fully concatenated feature vector

The proposed neural network architecture is presented in Table 3.2. The sizes of the hidden layers were selected to have 2^n multiples to simplify the computing effort. The neural network was coded as Python code and executed using Google Colaboratory tool to get the access to powerful GPUs capabilities, thereby reducing computational time.

3.7.2 Softmax classifier

The softmax is an activation function whose objective is to predict the instance's label in the training phase in categorizing multi-classes classifier. This function is employed as the last layer of a dense neural network by assigning a probability to each class. To converts the output vector,

Table 3.2 Proposed hidden layers

Layer	Input features	Output features
Hidden Layer 1	38,400	8,192
Hidden Layer 2	Dropout (25%)	
Hidden Layer 3	8,192	4,096
Hidden Layer 4	Dropout (25%)	
Hidden Layer 5	4,096	512
Softmax	512	8

from the numerical values into probabilities with range lies between [0,1] and sum equal to 1. The mathematical representation is expressed in the following Equation 3.4:

$$\sigma(z)_i = \frac{e_i^z}{\sum_{j=1}^{K} e_j^z} \tag{3.4}$$

Since the output vector from the dense neural network is subset from real numbers $z_i \in \mathbb{R}$, the exponential e_i^z function is applied to ensure that all the elements have positive values. Whereas $\sum_{j=1}^{K} e_j^z$ is a normalization term, creating a valid probability distribution with range (0, 1) and sum to 1.

3.7.3 Cross-entropy loss

Cross-entropy loss is a loss function that used in classification tasks. Zhang & Sabuncu (2018) explained the cross-entropy loss as an approach to quantifies the predicted output labels probability with true labels to enhance the likelihood of an event. Subsequently, improve the model's parameters by adjusting the weights parameters to minimize the loss. The multi-class cross-entropy loss function can be expressed as the negative summation between the true probability and the logarithm of predicted probability as follows:

$$Loss = -\sum_{n=1}^{N} y_n \times \log \hat{y}_n(x_i) \tag{3.5}$$

Whereas y_n presented the true label probability and $\hat{y}_n(x_i)$ the predicted class probability for a given example x_i. Penalizing the model more when it predicts low probabilities for the true class or high probabilities for the incorrect classes. Thereafter, any optimization algorithm can be used to minimize the cross-entropy loss function to enhance the model's performance.

3.8 Case Study: 3-bus System

This section presents a 3-bus system benchmark to test and validate the proposed classifier by generating, training, and testing the fault data.

3.8.1 Data Generation

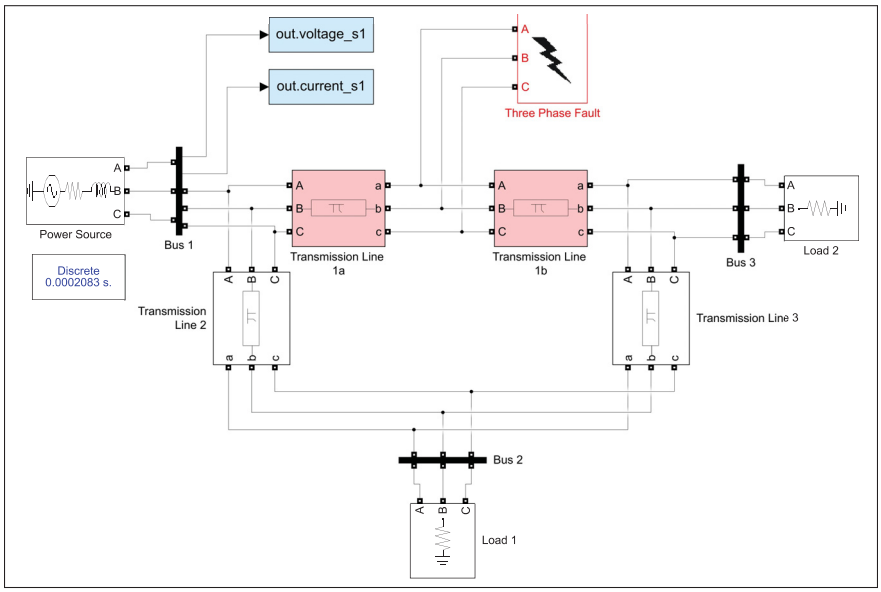

Figure 3.11 3-Bus system with fault occurred in line 1

Figure 3.11 illustrates the 3-bus system case study that is implemented in the research. The 3-bus system consists of: Three-phase transmission lines extended to distance of 200km and operating at 138kV, a 30 MVA generator as a power source connected to bus 1, and two loads with 10-20 MW connected to buses 2-3, respectively. The power flows through the transmission lines from bus 1 to feed the buses 2-3. The transmission lines have identical electrical characteristics as shown in Table 3.3.

In order to produce the data, the system was simulated multiple times to acquires the voltages and currents. The transmission line 1 is considered as the faulty line and is used to collect the measurement data from bus 1 using measurement tools from Simulink library. The measurements considered the phase-to-ground and Root Mean Square (RMS) for both voltages and currents.

The duration of simulation is 300 ms with fault occurred at t = 150 ms. The data are sampled at 4,800 samples per second (Hz). The fault location varied along the transmission line 1 to collect the data for at every 5 km interval, hence, the transmission lines were modelled as two separate three-phase PI section lines blocks with a sum equal to 200 km and three-phase fault block in the middle.

Consequently, each simulation generated 1,441 samples for each instance, totaling 8,646 data points for the voltage and current instances across all three phases. The simulated data are exported and saved as MATLAB Data format.

Various fault combinations were formed and simulated in between phases A, B, C, and ground, the detailed fault combination is presented in subsection 3.8.2.

Table 3.3 Transmission lines characteristics

	Resistances Ω/km		Inductance H/km		Capacitance F/km	
	Positive	Zero	Positive	Zero	Positive	Zero
Transmission Line 1,2,3	0.01273	0.3864	0.9337e-3	4.1264e-3	12.74e-9	7.751e-9

3.8.2 Dataset Labelling

The dataset in this research consists of different 8 classes distributed between normal and abnormal situations. Where the transmission lines could examine various types of faults between the phases or with grounds. This research considered both symmetrical faults such three-phase fault and asymmetrical faults such as single line-to-ground and double line-to-line faults and the normal operation without fault occurring.

Table 3.4 indicates the different fault combinations between the phases and the ground with the values of fault resistances. Additionally, to convert the categorical values into numerical format, the one-hot encoder transformed the class's label into one-of-K scheme.

Table 3.4 Fault classes and one-hot representation

Fault Type	Selected Phases	Fault Resistance	One-hot encoder
Single Line-to-Ground	A	0.001 Ω	[0,0,1,0,0,0,0,0]
Single Line-to-Ground	B	0.001 Ω	[0,0,0,0,1,0,0,0]
Single Line-to-Ground	C	0.001 Ω	[0,0,0,0,0,1,0,0]
Double Line-to-Line	A,B	0.001Ω	[1,0,0,0,0,0,0,0]
Double Line-to-Line	A,C	0.001Ω	[0,1,0,0,0,0,0,0]
Double Line-to-Line	B,C	0.001Ω	[0,0,0,1,0,0,0,0]
Three Phase Fault	A,B,C	0.001Ω	[0,0,0,0,0,0,1,0]
Normal Operation	–	–	[0,0,0,0,0,0,0,1]

3.8.3 Dataset Split

The dataset is divided into two main sets, the training set and test set as shown in Table 3.5. The training set represents 70% portion of the total dataset, whereas, the test set is 30%. Moreover, the training set is further divided into training sets and validation sets with fixed percentage 80% and 20%, respectively, to be able to implement the k-fold cross validation as discussed in previous Section 3.6.1.

Table 3.5 Distribution of dataset

Total number of images	Training set	Validation set	Test set
320	179	45	96

Since the data are distributed and shuffled randomly using built-in functions in Python, this ensures that the training and testing phases are based in a more representative and unbiased manner.

3.8.4 Setting the Neural Network Hyper-Parameters

To determine the neural network behavior and architecture, this section introduces the hyper-parameters that were settled in this research such as training by batches. Batching refers to dividing the training dataset into smaller batches. Thus, reducing the memory allocation and having faster convergence rates and lower computational time.

Additionally, the learning rate controls the model learning behavior after each iteration to update model's weights. Setting lower or higher learning rate can impact the training performance, as higher learning rates results faster convergence time; however, using higher learning rates carries the risk of potential divergence in the training process as it could overshoot the minimum. In contrast, lower learning rates have slower convergence to reach the minima with more precise adjustments to the model's weights.

The k-fold, dropout, activation function and pooling parameters were discussed in sections 3.6 and 3.5, receptively. The neural network hyper-parameters are summarized in the following Table 3.6.

Table 3.6 Proposed neural network hyper-parameters

Parameter	**Value**
Learning rate	0.000001
Number of K-fold	5 folds
Number of epoch	100
Batch size	4
Dropout rate	25%
Optimizer	Adam
Number of hidden layers	6 layers
Activation function	ReLU
Pooling	Max-pooling

3.8.5 Results and Discussion

The objective of the proposed classifier is to accurately classify and provide a general model to determine the fault type in the transmission lines or whether it is normal operation. This is possible using the neural networks proposed in the previous Section 3.7, where the objective function is to minimize the loss function using Adam optimizer.

Figure 3.12a,b shows the learning and loss curves over time, respectively. Whereas the learning curve depicts the model's accuracy behavior after each epoch, the loss curve illustrates the optimizer performance to minimize the objective function, Equation 3.5, to achieve the optimal weights by quantifying the losses during the training. Despite there are some fluctuations and variations in Figure 3.12b, the overall pattern indicates a decrease in the losses, hence, the optimizer is converging towards optimal values as the model continue training after each epoch.

Moreover, in the initial training phase, the model's accuracy increases rapidly, reaching 80% within 60 epochs. Subsequently, the learning curve shows a steady and gradual increase, eventually reaching approximately 89% in the last 40 epochs. This consistent improvement indicates that the learning process is approaching its saturation point before starts memorizing the training dataset and causing overfitting, consequently, the training process was stopped after 100 epochs.

3.8.5.1 Confusion and Performance Matrices

The evaluation process to determine the performance of the network model by assessing different criteria.

Confusion matrix is a heatmap that visualizes the relationship between the predicted and the actual labels in 2-dimensional axes. The x-axis represents the actual labels, whereas the predicted labels are in y-axis. The confusion matrix in Figure 3.13 shows the misclassifications in test set from actual label to wrong predicted label. In this case, a particular sample of a fault A&C was classified to fault B&C class.

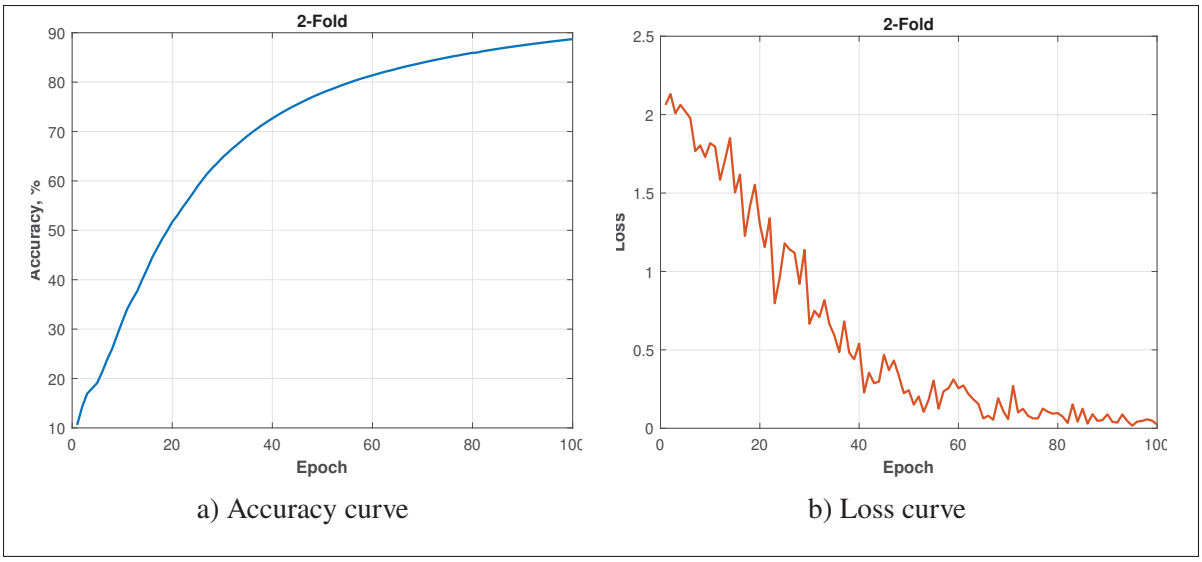

a) Accuracy curve b) Loss curve

Figure 3.12 2-fold in training process

The difference between the actual and the predicted values are analyzed using True Positive (TP), True Negative (TN), False Positive (FP), and False Negative (FN), using the following metrics:

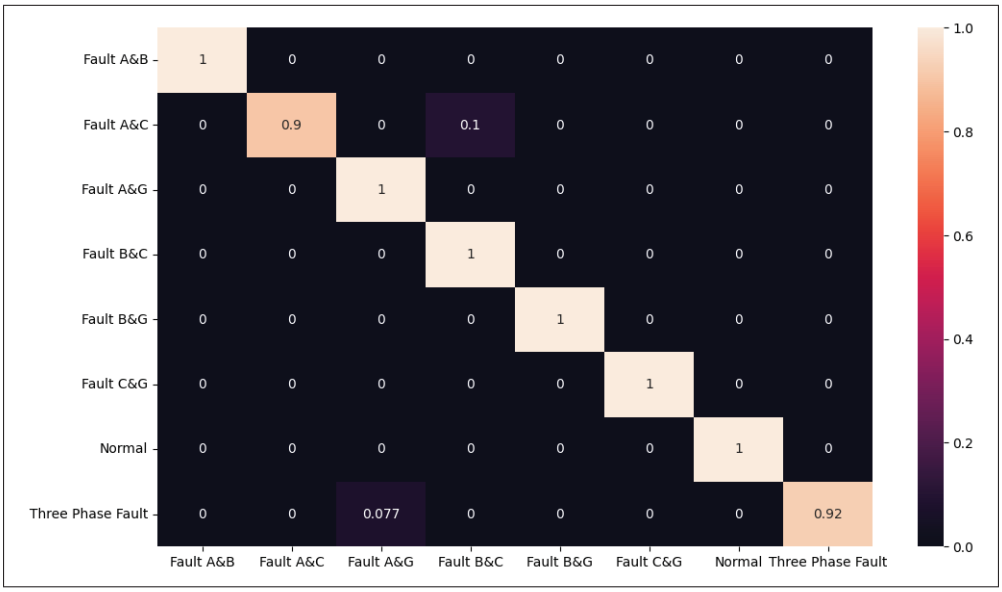

Figure 3.13 Predicted and true classes as confusion matrix

Accuracy: represents the percentage between the total predict values and the total true values as the following equation 3.6:

$$Accuracy = \frac{TP + TN}{TP + TN + FP + FN} \times 100 \tag{3.6}$$

After the model completed 100 epochs of training, the training accuracy for 5-folds were varying between 88.09% and 88.88% over 179 instances. Additionally, the validation accuracy was in between 95.5% and 100%, in this case, there are 2 instances that incorrectly classified or the total validation set is correctly classified. The summary was represented in Table 3.7. Whereas in test set, the trained neural network was able to classify 94 instance correctly. That represents a 97.9% of total test set.

Table 3.7 Training model's accuracy

Accuracy		
Fold	Training	Validation
1	88.09%	100%
2	88.71%	97.7%
3	88.78%	100%
4	87.89%	95.5%
5	88.88%	100%

Sensitivity quantifies how the model can detect the positive instances in multi-class situation as indicated in the following Equation 3.7:

$$Sensitivity = \frac{TP}{TP + FN} \tag{3.7}$$

Precision is a performance metric that measures how many correctly instances classified are relevant to the target class as shown in Equation 3.8:

$$Precision = \frac{TP}{TP + FP} \tag{3.8}$$

F1-score to measure the harmonic mean between the sensitivity and the precision in combined format as given in Equation 3.9

$$F1\text{-}score = \frac{2 \times precision \times sensitivity}{precision + sensitivity} \tag{3.9}$$

Table 3.8 compares the classifier's performance for each class based on the previous metrics. The fault A&G and fault B&C exhibit slightly lower precision scores of 0.94 and 0.92, respectively. In terms of sensitivity, it reveals a misclassifications correlation between the fault A&C and three phase fault classes for misclassifation.

Table 3.8 Performance of the classifier

Faults	Precision	Sensitivity	f1-score
Fault A&B	1.00	1.00	1.00
Fault A&C	1.00	0.90	0.95
Fault A&G	0.94	1.00	0.97
Fault B&C	0.92	1.00	0.96
Fault B&G	1.00	1.00	1.00
Fault C&G	1.00	1.00	1.00
Normal Operation	1.00	1.00	1.00
Three Phase Fault	1.00	0.92	0.96

3.8.5.2 Effects of Six-Phases Features on Accuracy

The explanation of the high accuracy results beside tuning model's hyper-parameters as shown in previous Section 3.8.4, is because of the similarity induced within the neural network. This occurs due to the presence of six phases, three phases for both voltages and currents.

Figure 3.14 illustrates the image's difference between fault A&B and fault B&C, when a fault occurs between phases A and B, phase C is slightly affected and maintains similar values

throughout the dataset to this specific fault for both the voltages and the currents, as Figure 3.4 shows.

Therefore, there are two feature vectors from both voltages and currents that remain unchanged for the unaffected phase, while the other four vectors will have more significant manner to the fully concatenated vector and to the classification task as discussed in Section 3.7. Consequently, two particular feature vectors remains constant during training.

However, this relies primarily on the selection of appropriate hyper-parameters and the architecture of the neural network. In different architecture, the classifier may reach saturation, causing the optimizer to struggle to converge. Thus, lose its ability to maintain the similarity propriety.

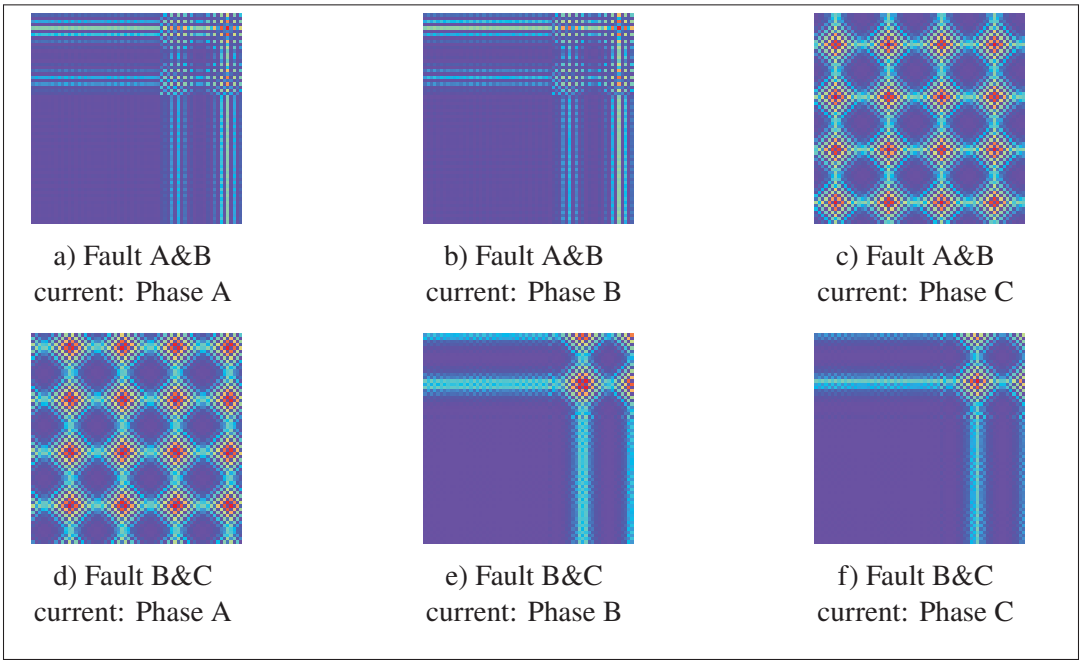

Figure 3.14 Comparing between fault A&B and fault B&C images

3.9 Conclusion

In conclusion, this chapter introduced a fault classifier that utilizes time-series transformation into images using GAF and employs CNN for feature extraction from these images. The proposed model was comprehensively described, encompassing various aspects such as an

overview of transmission line faults, the architecture of the fault classifier, feature extraction using convolutional layers, and measures to address overfitting.

Additionally, 3-bus case study was conducted to evaluate the performance of the proposed fault classifier model, achieving an impressive 97.9% classification accuracy on the test set. This outcome demonstrates the model's ability to accurately classify faults in transmission lines.

CHAPTER 4

OPTIMAL RELAY COORDINATION TIME

4.1 Introduction

In order to fulfill with the research's objective, this chapter will apply the methods outlined earlier for identifying relay pairs and fault classification. The 9-bus test system will be used for this purpose and subsequently determining the optimal replay coordination and compare the results with existing literature.

This chapter is structured as follows: Section 4.2 will outline the optimization problem by identifying the variables, constraints, and objective function. Section 4.3 will provide details about the 9-bus test system and present the results for each method. Lastly, the conclusion will be provided in Section 4.4.

4.2 Optimal Relay Coordination

The optimization is a mathematical operation where the main objective is to find the optimal solution for certain variables for an objective function by either minimize of maximize the objective function.

This section present the optimization for obtaining the optimal relay coordination time by obtaining the relay parameters that are discussed in Chapter 2. Specifically, the primary and backup relays will be coordinated to prevent any relay of misoperation. This coordination is achieved by short-circuit analysis, where the type of fault plays a crucial role in identifying the parameter I in Equation 2.2. The selection of variables, constraints and the objective function are discussed in the following subsections:

4.2.1 Optimization Variables

In an optimization problem, the design variables are the inputs or parameters that are being optimized. The design variables are the decision variables in the problem. The main objective is to identify the optimal values for these variables, which can involve either minimizing or maximizing them with respect to the objective function. However, the variables in this case may be integers or continues variables, hence, changing the optimization model.

In context of relay coordination, the optimization variables are the I_p and TDS, as mentioned in Chapter 2. While the values for TDS are defined as positive continuous variable, some literature such as Amraee (2012) and Zeienldin *et al.* (2004) proposed that I_p can be either discrete or continuous variable. In this research, the I_p is considered to be positive continuous variable.

4.2.2 Optimization Constraints

In addition to the variables, it is crucial to consider the constraints and the limitation associated with the optimization problem. These constraints help define a feasible region where optimal solutions can be discovered. Therefore, it is important to limit the optimization problem with constraints to enhance the feasibility of the solutions.

Coordination time interval, as discussed in Chapter 2, it is important to ensure the coordination between all the relays to be operative independently. According to Al-Roomi (2022), the CTI, time delay between primary and backup relays is indicated by the following expressions 4.1 with value 0.2 seconds:

$$T_{backup} - T_{primary} \geq CTI \tag{4.1}$$

Relay settings bounds is to guarantee that the relays operate within their designed operating settings. Each relay typically has settings of TDS and I_p that must be configured to ensure that the relays operate within their intended operational range. Hence, both TDS and I_p have minimum and maximum values that are expressed as inequality constraints in expressions 4.2

and 4.3, respectively.

$$TDS_{i,min} \leq TDS_i \leq TDS_{i,max} \tag{4.2}$$

$$Ip_{i,min} \leq Ip_i \leq Ip_{i,max} \tag{4.3}$$

The CTI value, as well as the minimum and maximum values of TDS and I_p, are defined according to the system's requirements. In this research, the minimum and maximum values of I_p and TDS are defined according to Alam *et al.* (2015) as the following Equations 4.4 and 4.5, respectively. $TDS_{i,min}$ is set to 0.1, whereas $TDS_{i,max}$ is set to 1.1.

$$Ip_{i,min} = max[0.5, min[1.25 \times I_{Lmax}, 1/3 \times I_{Fmin}]] \tag{4.4}$$

$$Ip_{i,max} = min[2.5, \frac{2}{3} \times I_{Fmin}] \tag{4.5}$$

Where I_{Lmax} is the maximum load current in the transmission lines and I_{Fmin} is the minimum fault current for a relay. Table 4.1 summarizes the minimum and maximum values of I_p for 9-bus test system, whereas ("see Appendix I, Table-A I-2") shows the I_{Lmax} and I_{Fmin} for the corresponding relays.

Table 4.1 Summary of relay I_p bounds

Relay	Ip_{min}	Ip_{max}	**Relay**	Ip_{min}	Ip_{max}
1	0.183	0.304	**13**	0.046	0.076
2	0.319	0.530	**14**	0.046	0.076
3	0.033	0.054	**15**	0.046	0.076
4	0.033	0.054	**16**	0.046	0.076
5	0.117	0.196	**17**	0.662	1.103
6	0.117	0.196	**18**	0.662	1.103
7	0.117	0.196	**19**	0.616	1.027
8	0.117	0.196	**20**	0.616	1.027
9	0.033	0.196	**21**	0.662	1.103
10	0.033	0.196	**22**	0.662	1.103
11	0.183	0.196	**23**	0.760	1.266
12	0.183	0.196	**24**	0.760	1.266

4.2.3 Objective Function

An objective function is a mathematical function that is used to describe the objective of an optimization problem, to find the optimal solution that satisfies all the constraints. In the context of this research, the objective function is a nonlinear mathematical function.

Equation 2.2 represents the operating time of a relay. Hence, the objective function is to minimize the total operating time across all the primary relays i in a power system protection is defined in the following Equation 4.6:

$$min \sum_{i=1} TDS_i \times \frac{A}{(\frac{I}{I_{pi}})^B - 1} \tag{4.6}$$

Consequently, the choice of an appropriate optimizer or algorithm is crucial to effectively support the nonlinear approach to find the optimal solution. In this research, the optimization is modeled as a Non-Linear Programming (NLP) and the chosen solver in GAMS was the CONOPT, utilizing Sequential Quadratic Programming (SQP) techniques.

4.3 Case Study: 9-Bus Test System

In this section, all the methods previously introduced in Chapter 2 and Chapter 3 are applied to a 9-bus system as part of the implementation process. The purpose of this implementation is to evaluate and test the effectiveness of the fault classification in the context of the 9-bus system. Furthermore, allowing for a more detailed performance optimization in comparison with existing literature in different fault scenarios.

To illustrate the identifying relays pairs in transmission line protection system and fault classification using proposed classifier in Chapter 3 , a 9-bus test system from Alam *et al.* (2015) is used as shown in Figure 4.1. As part of a 33kV transmission system, this test system consists of 12-transmission lines L1-L12 and one 100 MVA power source at bus 1.

The remaining buses are connected eight loads that are varied between 11.5MW and 3.3MW. All the 24-relays are DOCR type installed, with two opposite direction relays positioned at each transmission line.

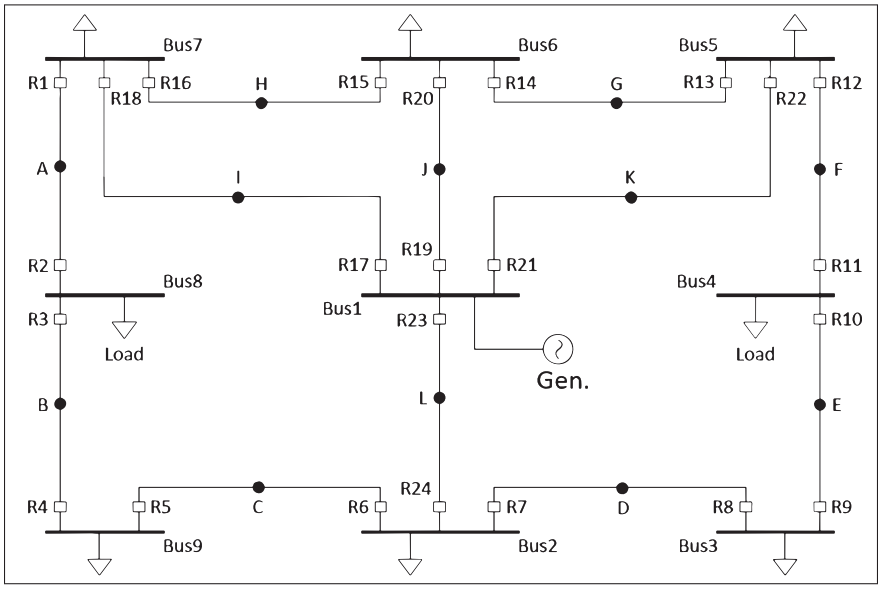

Figure 4.1 9-bus test system
Taken from Alam *et al.* (2015)

4.3.1 Identifying the Primary and the Backup Relays

The process of identifying the primary and backup relays is discussed in Chapter 2. Using LINKNET approach to determine the primary and the backup relays in 9-bus test system. The results of LINKNET are summarized in Table 4.2.

Although relays R17, R19, R21, and R23 have the sets of three backup relays for every individual relay, these backups cannot be utilized in the system due to certain constraints. The power source, which is located at bus 1, meaning that if a fault occurs at point "I", the primary relays responsible for rectify the fault are R17 and R18. The backup relays for R18 are provided in Table 4.2. However, in the case of R17, disconnecting R24 could result in an outage for bus 2. As a consequence, the remaining transmission lines could become overloaded, leading to unintended trips for the other relays and ultimately causing a blackout.

This scenario applies similarly to the backup relays R22 and R20. A similar scenario is also considered for R19, R21, and R23 due to their proximity to the generator.

Table 4.2 Primary and backup relay pairs for 9-bus test system

Primary Relay	**Backup Relay 1**	**Backup Relay 2**	**Primary Relay**	**Backup Relay 1**	**Backup Relay 2**	**Backup Relay 3**
1	17	15	**13**	21	11	—
2	4	—	**14**	19	16	—
3	1	—	**15**	19	13	—
4	6	—	**16**	17	2	—
5	3	—	**17**	24	22	20
6	23	8	**18**	15	2	—
7	23	5	**19**	24	20	18
8	10	—	**20**	16	13	—
9	7	—	**21**	24	20	18
10	12	—	**22**	14	11	—
11	9	—	**23**	22	20	18
12	21	14	**24**	8	5	—

4.3.2 Fault Classification

Figure 4.2 illustrates the 9-bus test system modelled in Simulink. Within this system, the line "I" is considered for fault classification using data acquired from measuring instruments installed at Bus 7. The line "I" is between bus 6 and bus 7, with a length of the transmission line 200 km and the transmission line modelled as two separate 'Three-Phase PI Section Line' block. To simulate faults occurring along the transmission line, in-line faults are produced at distances of 5 km, starting from near bus 6 and progressing towards bus 7. Consequently, a total of 40 faults are produced for each fault type.

Similar to Section 3.8, the faults in the dataset were sampled at a rate of 4,800 samples per second. The classification task is categorized into eight fault classes, and the dataset was divided into training, validation, and test sets. The size of each table is shown in Table 3.5 and fault classes are presented in Table 3.4.

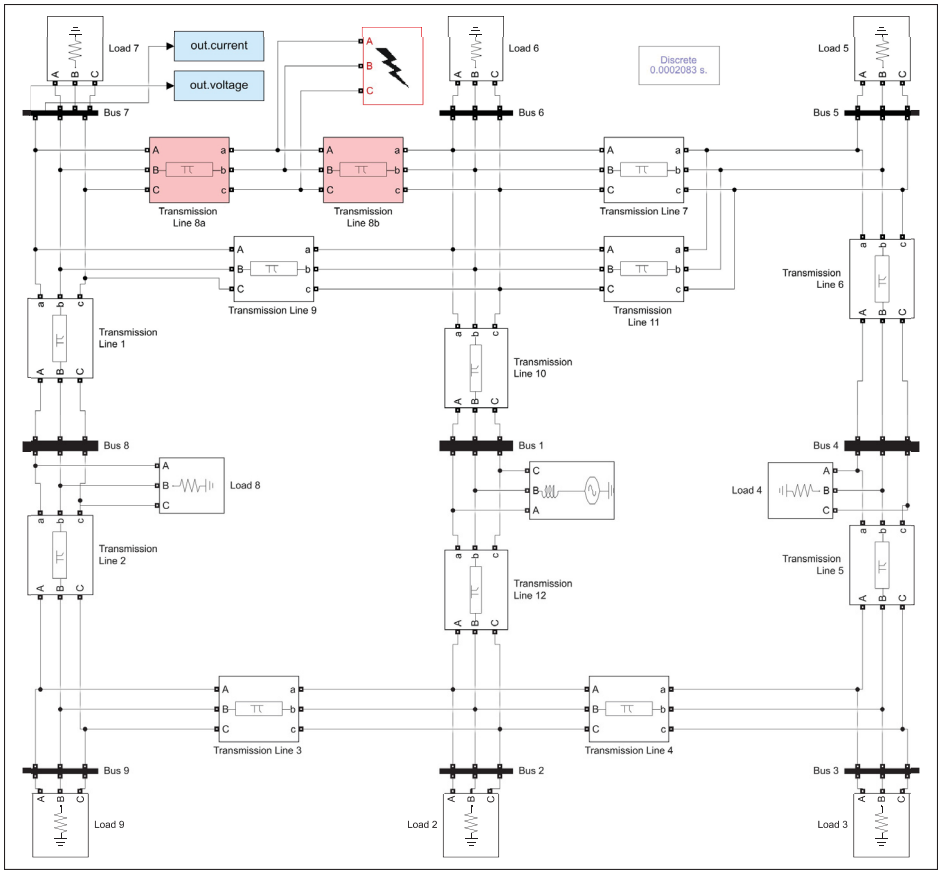

Figure 4.2 9-bus test system modelled in Simulink

Additionally, the neural network architecture implemented in the case study is identical to the one described in Section 3.5. The training process utilized a 5-fold approach, as explained in Section 3.6.1. Figure 4.3a illustrates the training accuracy over 100 epochs for each fold. The accuracy steadily increased, reaching approximately 90% by the end of each training iteration. Figure 4.3b represents the optimizer performance, the loss tended to decrease with fluctuations throughout the training process, indicating a convergence.

As a result of the training process, the performance of the classifier was evaluated using the test dataset, and the outcomes are depicted as a confusion matrix in Figure 4.4. Remarkably, the classifier achieved exceptional accuracy by successfully identifying all 96 fault instances in the test dataset. This outcome shows the proposed neural network performance of accurately classify and detect faults in the 9-bus system.

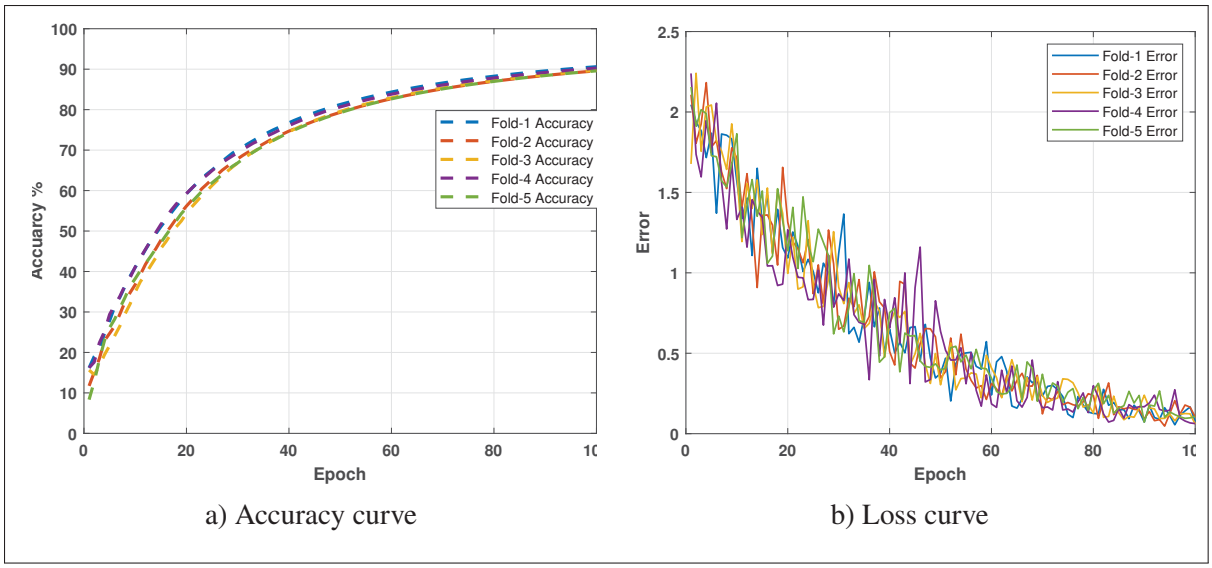

a) Accuracy curve b) Loss curve

Figure 4.3 Training curves of the 9-bus test system

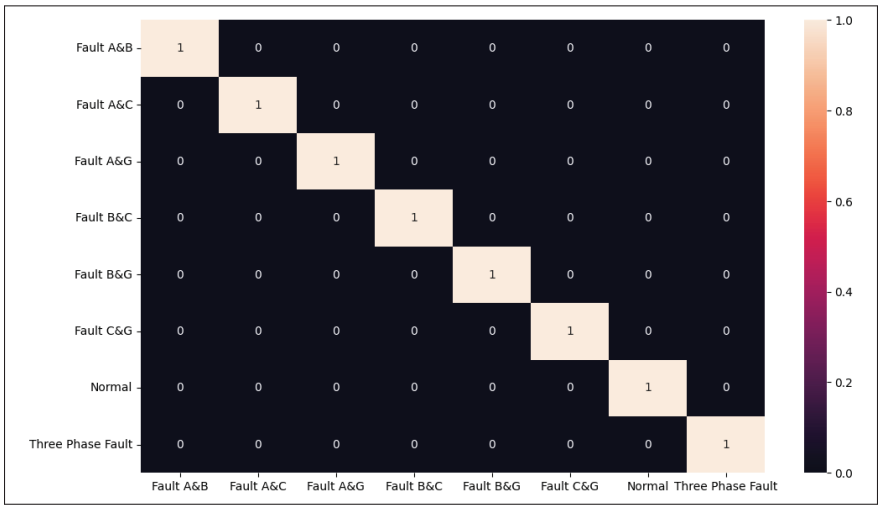

Figure 4.4 The results as confusion matrix for 9-bus test system

Moreover, when the signal is acquired from bus 7, it clearly reveals the presence of faults and enabling the fault to be easily detected from this particular bus. A comparison between the voltage signals acquired from bus 7 and bus 1 is presented in Figure 4.5. In Figure 4.5a, it is evident that bus 7 provides a clear view of the fault that occurred at t=0.15s, whereas bus 1 in Figure 4.5 lacks the necessary detail to observe the fault signal.

However, when acquiring data from bus 1, voltage and current signals appears similar for all different fault classes as shown ("see Appendix I, Figure-A I-2"), making it challenging for the classifier to differentiate between the faults. Similarly, when the signals obtained from bus 6, the appearance of the fault in the signal is not clear as shown ("see Appendix I, Figure-A I-3"). Therefore, the choice of the bus from which the signal is acquired is crucial, as it directly impacts the clarity and sensitivity of the signal, thereby affecting the transforming time-series to an image and classifier's performance accordingly.

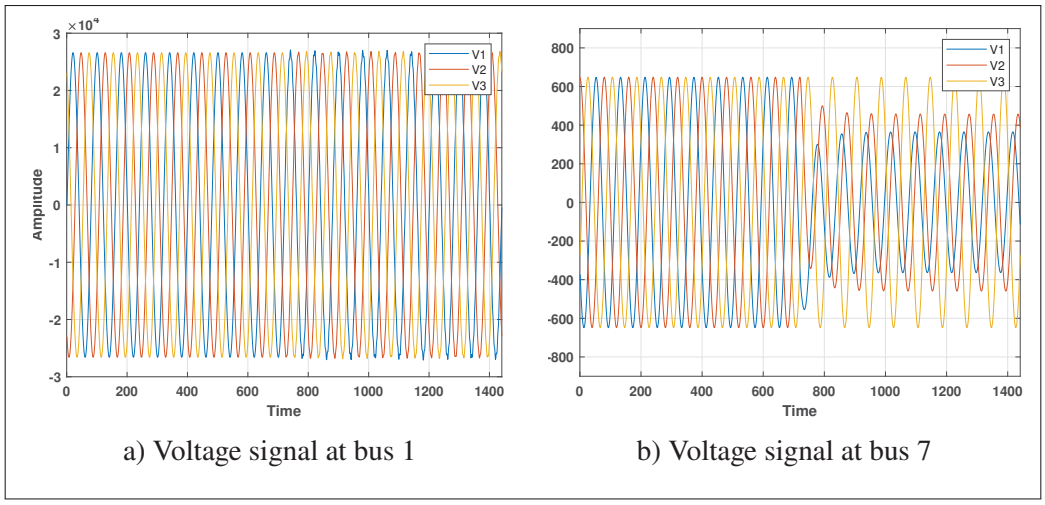

a) Voltage signal at bus 1 b) Voltage signal at bus 7

Figure 4.5 Comparison between voltage signals acquired from two buses

4.3.3 Relay Coordination

After the fault classification process, the final step in this research is to obtain the optimal relay coordination, where both primary and backup relays must be coordinated together, as described in Section 4.2, using the GAMS software to solve the objective function in Equation 4.6. The optimization solutions are compared with those given in Alam *et al.* (2015) in Table 4.3. In this research, the GAMS was used to obtain the total primary operating time of 10.973s, which outperforms other methods such as GA, Particle Swarm Optimization (PSO), and Seeker Optimization Algorithm (SOA) to find the minimum total primary relay operating time. However, Differential Evolution (DE) and Harmony Search (HS) were able to enhance the optimization

problem further, achieving a lower total operating time of 8.6822s in DE. Despite, GAMS still demonstrates a faster time to reach the optimal solution compared to all other methods.

Table 4.3 Comparison between different optimization approaches

	GA	PSO	DE	HS	SOA	CONOPT
Objective function	14.5426	13.9472	8.6822	9.2339	14.2238	10.973
Elapse time (s)	314.44	3.97	15.06	155.56	33.74	0.047

Figure 4.6 illustrates the values of TDS and I_p for the different optimization methods in Alam *et al.* (2015). It is evident that the GAMS algorithm, along with DE and HS methods, successfully maintains the lowest value of TDS, as shown in Figure 4.6a. However, in finding the optimal value for I_p, the GAMS approach fluctuates between the minimum and maximum constraints, similar to GA, PSO, and SOA as depicted in Figure 4.6b. Detailed optimal values for TDS and I_p are provided ("see Appendix I, Table-A I-3").

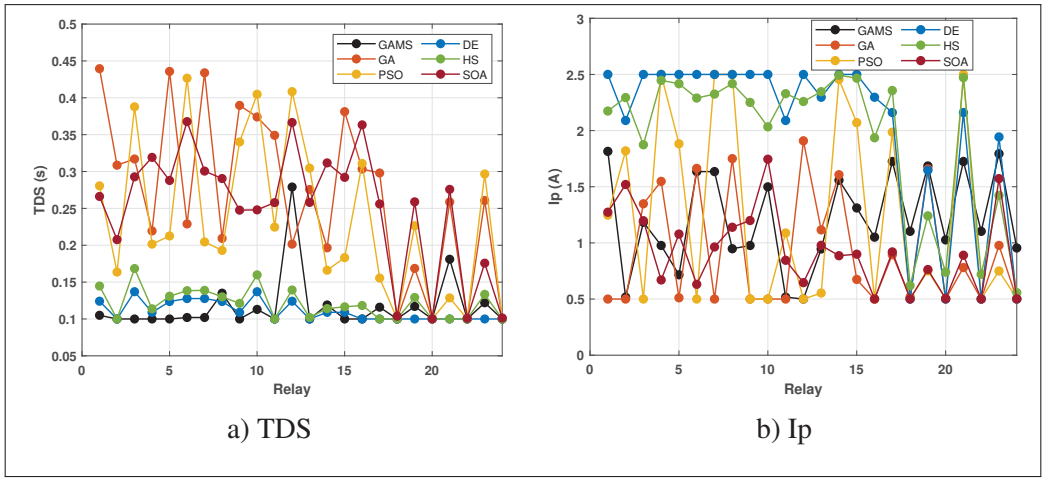

a) TDS b) Ip

Figure 4.6 Comparison between the optimization methods

Once faults are classified, it becomes crucial to coordinate the relays based on the type of the fault.This ensures that the relays respond differently to each fault scenario, depending on the nature of the fault. GAMS offers the advantage of generating optimal coordination in less time, allowing for adaptive changes in relay's parameters more rapidly in context to those given in Alam (2019). Figure 4.7 demonstrates different CTI values for various faults conditions as SLG,

L-L, and Three-Phase faults that occurred in line 'I' of the 9-bus system. The primary relay R15, along with backup relays R19 and R13, as well as the primary relay R16 with R2 and R17, adapt their parameters (TDS, I_p) according to fault types. However, the remaining relays maintain their original parameters.

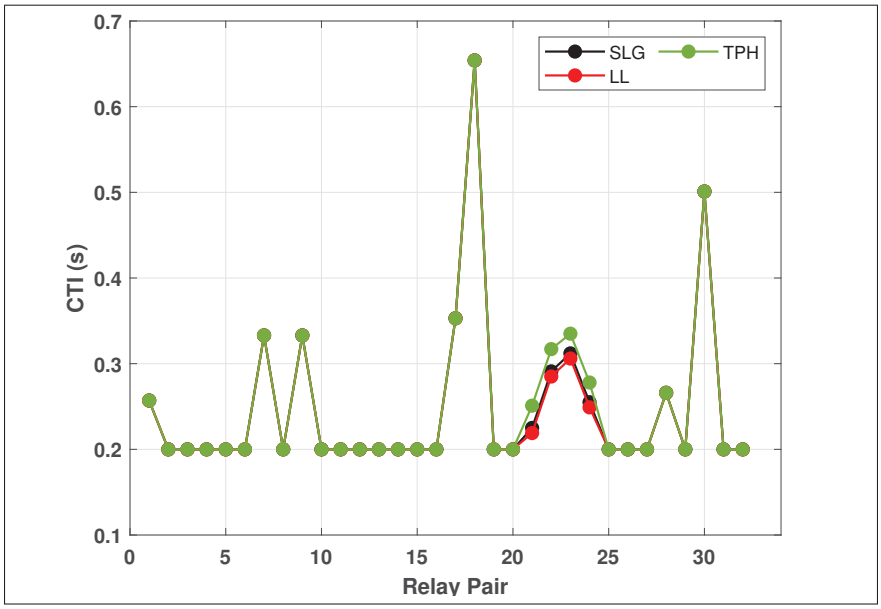

Figure 4.7 Different CTI values for the relay pairs

4.4 Conclusion

In conclusion, to achieve the research objective, this chapter implemented the previously methods for identifying relay pairs and the model for classifying faults. The 9-bus test system is used to examine these approach. Furthermore, model the relay coordination as optimization problem and find the optimal relay's parameters using GAMS and compare the results with existing literature. Lastly, change the relay's parameters according to fault type to enhance the CTI and decrease the relay operating time.

CONCLUSION AND RECOMMENDATIONS

In conclusion, this research discussed the importance of identifying primary and backup relays for the transmission lines. As the primary relays initiate responses to faults in transmission lines, while backup relays provide an additional layer of protection in case the primary relays fail. The utilization of the LINKNET approach, along with the List and Next vectors, enables the method to identify the relay pairs for a transmission line. Besides, controls the operating time by introducing the inverse-time directional overcurrent relays by customized the relay's parameters according to time-current curve. The CTI parameter is particularly important as it represents the time delay between the activation of primary and backup relays. Ensuring that the primary relay operates first and the backup relay intervenes only if the primary relay fails within the designated time is critical.

Furthermore, introducing a fault classifier that transforms time-series data into images using GAF and applies CNN for feature extraction. The voltage and current signals were transformed into 224px images to be complied with the AlexNet architecture for feature extractions. The features from the images were concatenated into a signal vector to be ready to feed it into six-hidden layers of fully connected layers. The proposed model was described comprehensively, covering aspects such as an overview of transmission line faults and addressing the solution for overfitting. A case study on a 3-bus system demonstrates the proposed fault classifier's impressive 97.9% accuracy in classifying eight transmission line faults.

To achieve the research objective, a 9-bus test system was implemented to examine the overall previously discussed methods for identifying relay pairs and the fault classification model. Furthermore, the relay coordination was modeled as an optimization problem, by defining the constraints for relay's parameters and formulate the objective functions as minimizing the total operating time for all primary relays. Using GAMS software, the optimization results of the objective function were compared with existing literature. Eventually, the CONOPT approach

in GAMS software outperform the time elapsed to obtain the local minima for the objective function in 0.047 seconds, in comparison to PSO 83.4 % less time, while by with DE and HS finds the optimal solution in 15.06 and 9.233 seconds, respectively. Finally, the relay parameters were adjusted according to the fault type to enhance the CTI and reduce the relay operating time. Overall, the combined efforts of identifying relay pairs, implementing fault classification models, and optimizing relay coordination parameters contribute to the efficient and accurate protection of power systems, minimizing false tripping and ensuring reliable operation.

5.1 Recommendations for Future Works

As the fault classifier is used to classify the fault within the transmission lines, there is a need to improve the classifier to create more adaptive power system protection. Therefore, the future work includes:

- Extend the classifier to find the location of the faults to increase the versatility in classifying both the location and type of faults within a power system.
- Evaluate the classifier by introducing artificial noise to the images and during training, allowing it to learn and adapt to noisy conditions.
- Optimize the selection of data acquisition locations to identify the most suitable positions for gathering data. This approach minimize the number of measurement tools required and reduce the input data, thereby enhancing the performance of the fault classifier.
- Integrate communication protocols like IEC 61850 to facilitate enhanced communication between relays, allowing for instance modification of relay parameters. This enables more efficient and immediate adjustment of relay settings.
- Develop real-time monitoring and control capabilities to enable proactive fault management. This could involve implementing the proposed fault classifier that can detect and respond to faults in real-time, enabling swift corrective actions to power system protection.

- Develop real-time monitoring and control capabilities to enable proactive fault management. This could involve implementing the proposed fault classifier that can detect and respond to faults in real-time, enabling swift corrective actions to power system protection.
- Explore the possibility of utilizing the raw signals directly. For instance, employing approaches such as 1D-CNN, combined CNN and LSTM, and SVM for fault classification and compare the performance between the classifiers.

APPENDIX I

SUPPORTING MATERIALS

1. Supporting Materials for Chapter 2

Figure-A I-1a,b represents the Block X and Block Y in LINKNET methods, where these flowcharts assist Figure 2.3 to determine the relay pairs.

Table-A I-1 shows the LINKNET structure for the 6-bus system as explained Chapter 2 with detail about the List, Far, Next , and End vectors.

Table-A I-1 The detailed List and vectors for LINKNET structure for 5-bus system

Line	Relay	Opposite Bus	End	List		Far (Relay)	Next
Line 1	1	2	1	List 2	1	1	0
	2	1	2	List 1	2	2	0
Line 2	3	3	3	List 3	3	1	0
	4	1	5	List 1	4	3	2
Line 3	5	3	5	List 3	5	2	3
	6	2	6	List 2	6	3	1
Line 4	7	4	7	List 4	7	2	0
	8	2	8	List 2	8	4	6
Line 5	9	5	9	List 5	9	2	0
	10	2	10	List 2	10	5	8
Line 6	11	4	11	List 4	11	3	7
	12	3	12	List 3	12	4	5
Line 7	13	5	13	List 5	13	4	9
	14	4	14	List 4	14	5	11

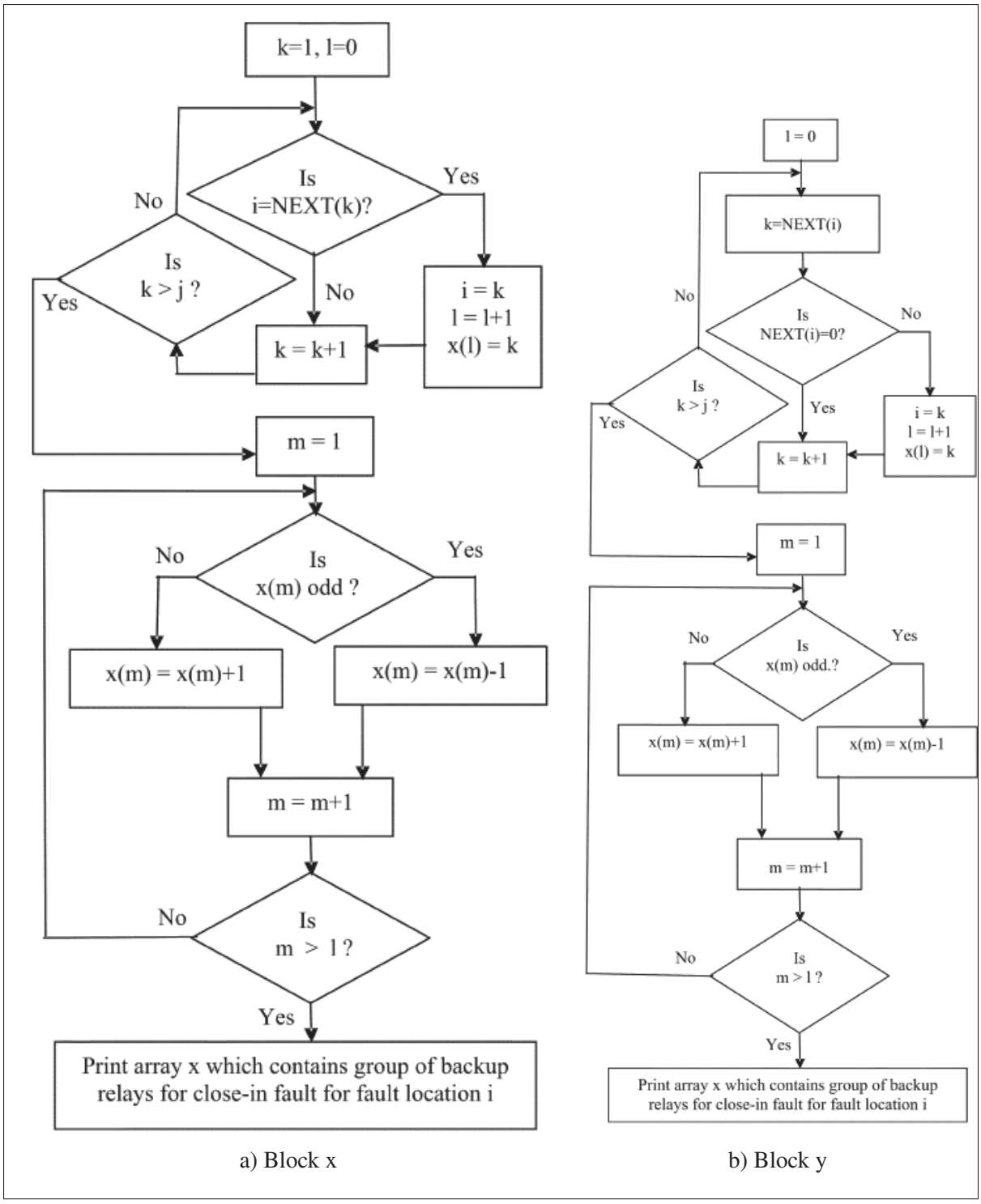

Figure-A I-1 Block x and Block Y as part of LINKNET structure
Taken from Birla *et al.* (2004)

2. Supporting Materials for Chapter 4

Figure-A I-2, I-3, and I-4 illustrates the voltage and current signal acquired from bus 1, bus 6, and bus 7, respectively. These signals were obtained in Three-Phase fault in L8 in 9-bus system, further details are explained in Chapter 4.

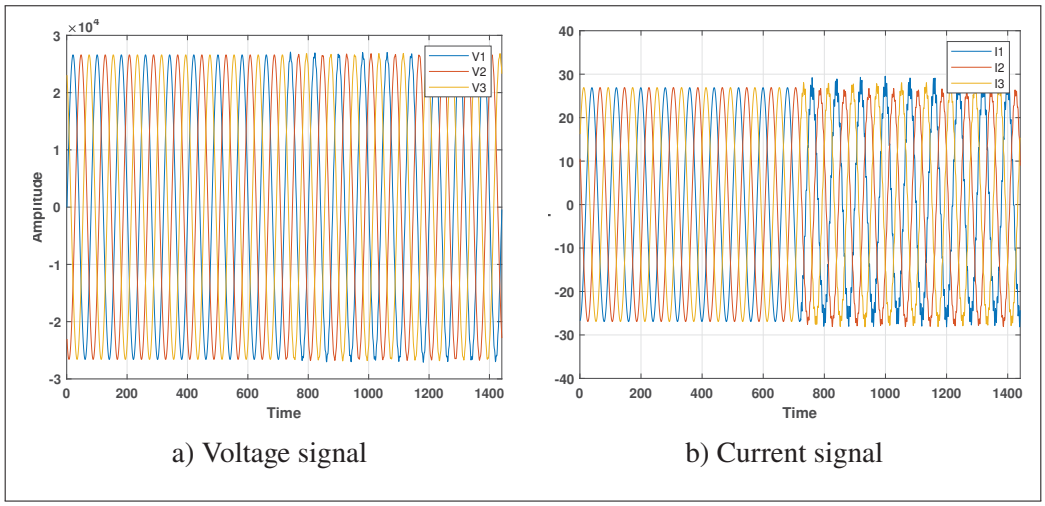

a) Voltage signal b) Current signal

Figure-A I-2 Voltage and current signals acquired from bus 1

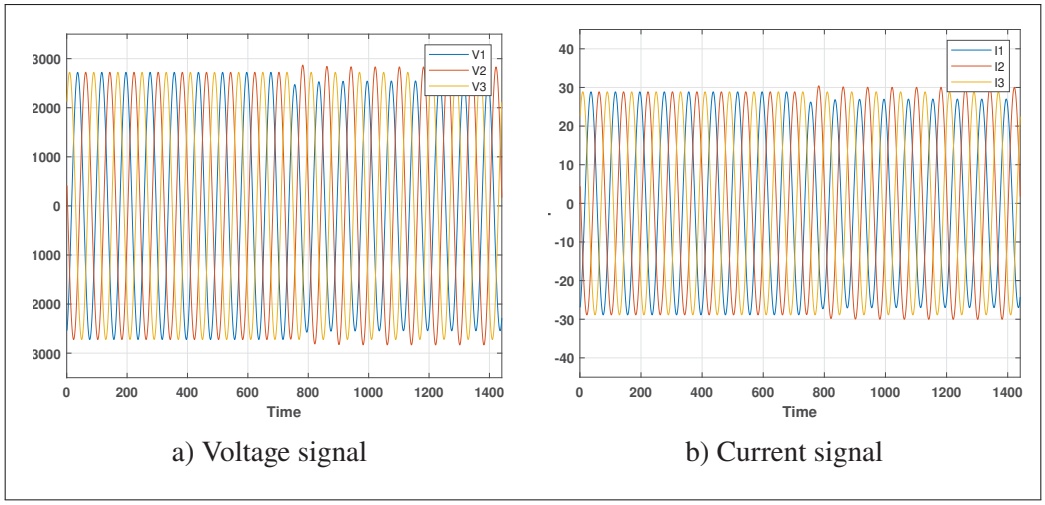

a) Voltage signal b) Current signal

Figure-A I-3 Voltage and current signals acquired from bus 6

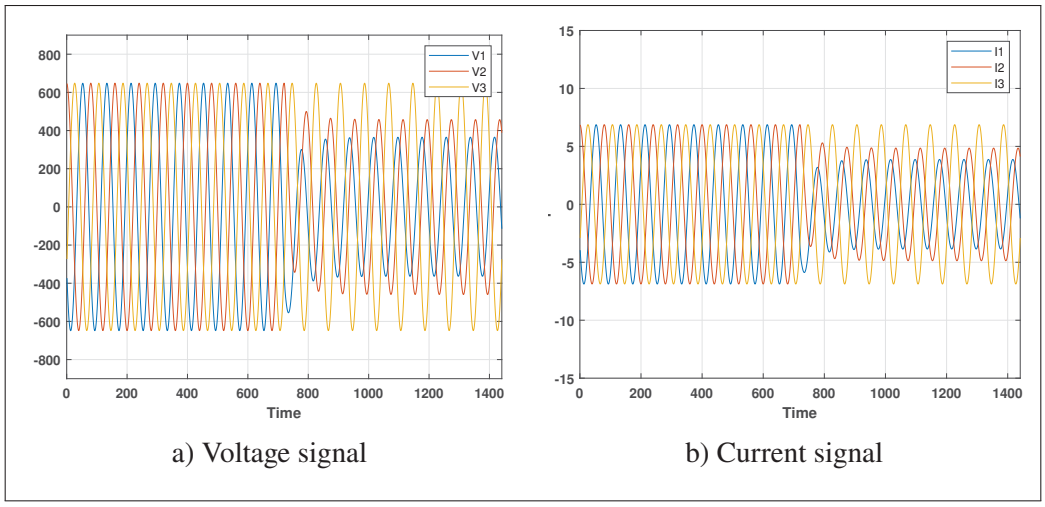

a) Voltage signal b) Current signal

Figure-A I-4 Voltage and current signals acquired from bus 7

Table-A I-2 shows the I_{Lmax} and I_{Fmin} bounds for a corresponding relay. These values are essential to determine the optimal relay setting as they represents the constraints for the optimization problem.

Table-A I-2 Summary of I_{Lmax} and I_{Fmin} bounds
Taken from Al-Roomi (2022)

Relay	I_{Lmax}	Ip_{max}	**Relay**	I_{Lmax}	I_{Fmin}
1	121.74	1361.6	**13**	30.44	1031.7
2	212.74	653.6	**14**	30.44	1168.3
3	21.74	1124.4	**15**	30.44	1168.3
4	21.74	1044.2	**16**	30.44	1031.7
5	78.26	711.2	**17**	411.3	1293.9
6	78.26	1226	**18**	411.3	1953.7
7	78.26	1226	**19**	410.87	1264.1
8	78.26	711.2	**20**	410.87	2256.8
9	21.74	1044.2	**21**	441.3	1293.9
10	21.74	1124.4	**22**	441.3	1953.7
11	121.74	653.6	**23**	506.52	1345.5
12	121.74	787.2	**24**	506.52	1432.3

In Table-A I-3 shows the optimal TDS and I_P values for all relays in 9-bus test system using GAMS.

Table-A I-3 Obtained TDS and I_P using GAMS

Relay	**TDS**	**Ip**	**Relay**	**TDS**	**IP**
1	0.105	1.815	**13**	0.1	0.946
2	0.1	0.517	**14**	0.119	1.558
3	0.1	1.184	**15**	0.1	1.311
4	0.1	0.977	**16**	0.1	1.051
5	0.1	0.716	**17**	0.116	1.725
6	0.102	1.635	**18**	0.1	1.103
7	0.102	1.635	**19**	0.117	1.685
8	0.135	0.948	**20**	0.1	1.027
9	0.1	0.977	**21**	0.181	1.725
10	0.113	1.499	**22**	0.1	1.103
11	0.1	0.517	**23**	0.122	1.794
12	0.279	0.5	**24**	0.1	0.955

Whereas Tables-A I-4, I-5, and I-6, summarized the CTI values between the primary and backup relay in 9-bus system for Single-Line-Ground fault, Line-to-Line fault, Three Phase Fault situations.

Table-A I-4 Summary of CTI between the primary and backup relay I_p for 9-bus system in SLG fault situation

Primary Relay	Backup Relay	CTI	**Primary Relay**	Backup Relay	CTI
1	15	0.257	13	11	0.353
1	17	0.2	13	21	0.654
2	4	0.2	14	16	0.2
3	1	0.2	14	19	0.2
4	6	0.2	15	13	0.225
5	3	0.2	15	17	0.291
6	8	0.333	16	2	0.312
6	23	0.2	16	17	0.255
7	5	0.2	18	2	0.2
7	23	0.2	18	15	0.2
8	1	0.2	20	13	0.2
9	7	0.2	20	16	0.266
10	12	0.2	22	11	0.2
11	9	0.2	22	14	0.501
12	14	0.2	24	5	0.2
12	21	0.2	24	8	0.2

Table-A I-5 Summary of CTI between the primary and backup relay I_p for 9-bus system in LL fault situation

Primary Relay	Backup Relay	CTI	**Primary Relay**	Backup Relay	CTI
1	15	0.257	13	11	0.353
1	17	0.2	13	21	0.654
2	4	0.2	14	16	0.2
3	1	0.2	14	19	0.2
4	6	0.2	15	13	0.219
5	3	0.2	15	17	0.285
6	8	0.333	16	2	0.306
6	23	0.2	16	17	0.249
7	5	0.2	18	2	0.2
7	23	0.2	18	15	0.2
8	1	0.2	20	13	0.2
9	7	0.2	20	16	0.266
10	12	0.2	22	11	0.2
11	9	0.2	22	14	0.501
12	14	0.2	24	5	0.2
12	21	0.2	24	8	0.2

Table-A I-6 Summary of CTI between the primary and backup relay I_p for 9-bus system in Three-Phase fault situation

Primary Relay	Backup Relay	CTI	**Primary Relay**	Backup Relay	CTI
1	15	0.257	13	11	0.353
1	17	0.2	13	21	0.654
2	4	0.2	14	16	0.2
3	1	0.2	14	19	0.2
4	6	0.2	15	13	0.251
5	3	0.2	15	17	0.317
6	8	0.333	16	2	0.335
6	23	0.2	16	17	0.278
7	5	0.2	18	2	0.2
7	23	0.2	18	15	0.2
8	1	0.2	20	13	0.2
9	7	0.2	20	16	0.266
10	12	0.2	22	11	0.2
11	9	0.2	22	14	0.501
12	14	0.2	24	5	0.2
12	21	0.2	24	8	0.2

Table-A I-7 The detailed List and vectors for LINKNET structure for 9-bus system

Line	Relay	Opposite Bus	End	List		Far (Relay)	Next
Line 1	1	8	1	List 8	1	7	0
	2	7	2	List 7	2	8	0
Line 2	3	9	3	List 9	3	8	0
	4	8	5	List 8	4	9	0
Line 3	5	2	5	List 2	5	9	0
	6	9	6	List 9	6	2	3
Line 4	7	3	7	List 3	7	2	0
	8	2	8	List 2	8	3	5
Line 5	9	4	9	List 4	9	3	0
	10	3	10	List 3	10	4	7
Line 6	11	5	11	List 5	11	4	0
	12	4	12	List 4	12	5	9
Line 7	13	6	13	List 6	13	5	0
	14	5	14	List 5	14	6	11
Line 8	15	7	15	List 7	15	6	2
	16	6	16	List 6	16	7	13
Line 9	17	7	17	List 7	17	1	15
	18	1	18	List 1	18	7	0
Line 10	19	6	19	List 6	19	1	16
	20	1	20	List 1	20	6	18
Line 11	21	5	21	List 5	21	1	14
	22	1	22	List 1	22	5	20
Line 12	23	2	23	List 2	23	1	8
	24	1	24	List 1	24	2	22

BIBLIOGRAPHY

Acharya, D. & Das, D. K. (2022). An efficient optimizer for optimal overcurrent relay coordination in power distribution system. *Expert Systems with Applications*, 199, 116858. doi: https://doi.org/10.1016/j.eswa.2022.116858.

Adelnia, F., Moravej, Z. & Farzinfar, M. (2015). A new formulation for coordination of directional overcurrent relays in interconnected networks. *International Transactions on Electrical Energy Systems*, 25(1), 120-137. doi: https://doi.org/10.1002/etep.1828.

Akdag, O. & Yeroglu, C. (2021). Optimal directional overcurrent relay coordination using MRFO algorithm: A case study of adaptive protection of the distribution network of the Hatay province of Turkey. *Electric Power Systems Research*, 192, 106998. doi: https://doi.org/10.1016/j.epsr.2020.106998.

Al-Roomi, A. R. (2022). Directional Overcurrent Relays and the Importance of Relay Coordination. In *Optimal Coordination of Power Protective Devices with Illustrative Examples* (pp. 139-167). doi: 10.1002/9781119794929.ch5.

Alaee, P. & Amraee, T. (2021). Optimal Coordination of Directional Overcurrent Relays in Meshed Active Distribution Network Using Imperialistic Competition Algorithm. *Journal of Modern Power Systems and Clean Energy*, 9(2), 416-422. doi: 10.35833/MPCE.2019.000184.

Alam, M. N. (2019). Adaptive Protection Coordination Scheme Using Numerical Directional Overcurrent Relays. *IEEE Transactions on Industrial Informatics*, 15(1), 64-73. doi: 10.1109/TII.2018.2834474.

Alam, M. N., Das, B. & Pant, V. (2015). A comparative study of metaheuristic optimization approaches for directional overcurrent relays coordination. *Electric Power Systems Research*, 128, 39-52. doi: https://doi.org/10.1016/j.epsr.2015.06.018.

Albawi, S., Mohammed, T. A. & Al-Zawi, S. (2017). Understanding of a convolutional neural network. *2017 International Conference on Engineering and Technology (ICET)*, pp. 1-6. doi: 10.1109/ICEngTechnol.2017.8308186.

Amraee, T. (2012). Coordination of Directional Overcurrent Relays Using Seeker Algorithm. *IEEE Transactions on Power Delivery*, 27(3), 1415-1422. doi: 10.1109/TPWRD.2012.2190107.

Ates, Y., Uzunoglu, M., Karakas, A., Boynuegri, A. R., Nadar, A. & Dag, B. (2016). Implementation of adaptive relay coordination in distribution systems including distributed generation. *Journal of Cleaner Production*, 112, 2697-2705. doi: https://doi.org/10.1016/j.jclepro.2015.10.066.

Atteya, A. I., El Zonkoly, A. M. & Ashour, H. A. (2017). Optimal relay coordination of an adaptive protection scheme using modified PSO algorithm. *2017 Nineteenth International Middle East Power Systems Conference (MEPCON)*, pp. 689-694. doi: 10.1109/MEPCON.2017.8301256.

Birla, D., Maheshwari, R. & Gupta, H. (2004). Novel technique for relay pair identification: a relay coordination requirement. *2004 IIT 13th National Power System Conference*.

Bishop, P. & Nair, N. K. C. (2023). *IEC 61850 principles and applications to electric power systems* (ed. Second edition.). Cham: Springer. doi: 10.1007/978-3-031-24567-1.

Breiman, L. (2001). Random Forests. *Machine Learning*, 45(1), 5-32. doi: 10.1023/A:1010933404324.

Chakraborty, D., Sur, U. & Banerjee, P. K. (2019). Random Forest Based Fault Classification Technique for Active Power System Networks. *2019 IEEE International WIE Conference on Electrical and Computer Engineering (WIECON-ECE)*, pp. 1-4. doi: 10.1109/WIECON-ECE48653.2019.9019922.

Coffele, F., Booth, C. & Dyśko, A. (2015). An Adaptive Overcurrent Protection Scheme for Distribution Networks. *IEEE Transactions on Power Delivery*, 30(2), 561-568. doi: 10.1109/TPWRD.2013.2294879.

El-Fergany, A. (2016). Optimal directional digital overcurrent relays coordination and arc-flash hazard assessments in meshed networks. *International Transactions on Electrical Energy Systems*, 26(1), 134-154. doi: https://doi.org/10.1002/etep.2073.

El-Hamrawy, A. H., Ebrahiem, A. A. M. & Megahed, A. I. (2022). Improved Adaptive Protection Scheme Based Combined Centralized/Decentralized Communications for Power Systems Equipped With Distributed Generation. *IEEE Access*, 10, 97061-97074. doi: 10.1109/ACCESS.2022.3205312.

Elnozahy, A., Sayed, K. & Bahyeldin, M. (2019). Artificial Neural Network Based Fault Classification and Location for Transmission Lines. *2019 IEEE Conference on Power Electronics and Renewable Energy (CPERE)*, pp. 140-144. doi: 10.1109/CPERE45374.2019.8980173.

Fani, B., Dadkhah, M. & Karami-Horestani, A. (2018). Adaptive protection coordination scheme against the staircase fault current waveforms in PV-dominated distribution systems. *IET Generation, Transmission & Distribution*, 12(9), 2065-2071. doi: https://doi.org/10.1049/iet-gtd.2017.0586.

Faria, W. R., de B. Martins, D., Nametala, C. A. & Pereira, B. R. (2020). Protection system planning for distribution networks: A probabilistic approach. *Electric Power Systems Research*, 189, 106612. doi: https://doi.org/10.1016/j.epsr.2020.106612.

Fonseca, G. A., Ferreira, D. D., Costa, F. B. & Almeida, A. R. (2022). Fault Classification in Transmission Lines Using Random Forest and Notch Filter. *Journal of Control, Automation and Electrical Systems*, 33(2), 598-609. doi: 10.1007/s40313-021-00844-4.

GAMS, C. D. (2023). General Algebraic Mdeling System (Version 24.8.3) [Software]. Germany: GAMS Software GmbH.

Glover, J. D., Sarma, M. S. . & Overbye, T. J. T. J. (2012). *Power system analysis and design* (ed. 5th ed.). Stamford, CT: Cengage Learning. Retrieved from: http://catdir.loc.gov/catdir/toc/fy12pdf01/2010941448.html.

Gu, J., Wang, Z., Kuen, J., Ma, L., Shahroudy, A., Shuai, B., Liu, T., Wang, X., Wang, G., Cai, J. & Chen, T. (2018). Recent advances in convolutional neural networks. *Pattern Recognition*, 77, 354-377. doi: https://doi.org/10.1016/j.patcog.2017.10.013.

Jamil, M., Sharma, S. K. & Singh, R. (2015). Fault detection and classification in electrical power transmission system using artificial neural network. *SpringerPlus*, 4(1), 334. doi: 10.1186/s40064-015-1080-x.

Khurshaid, T., Wadood, A., Gholami Farkoush, S., Kim, C.-H., Yu, J. & Rhee, S.-B. (2019). Improved Firefly Algorithm for the Optimal Coordination of Directional Overcurrent Relays. *IEEE Access*, 7, 78503-78514. doi: 10.1109/ACCESS.2019.2922426.

Krizhevsky, A., Sutskever, I. & Hinton, G. E. (2017). Imagenet classification with deep convolutional neural networks. *Communications of the ACM*, 60(6), 84–90.

Kumar, D. S. & Srinivasan, D. (2018). A Numerical Protection Strategy for Medium-Voltage Distribution Systems. *2018 IEEE Innovative Smart Grid Technologies - Asia (ISGT Asia)*, pp. 1056-1061. doi: 10.1109/ISGT-Asia.2018.8467835.

Lahiri, U., Pradhan, A. & Mukhopadhyaya, S. (2005). Modular neural network-based directional relay for transmission line protection. *IEEE Transactions on Power Systems*, 20(4), 2154-2155. doi: 10.1109/TPWRS.2005.857839.

Laway, N. & Gupta, H. (1994). An efficient method for generation, storage and retrieval of data for the coordination of directional relays. *Electric Power Systems Research*, 29(2), 147-152. doi: https://doi.org/10.1016/0378-7796(94)90072-8.

Lecun, Y., Bottou, L., Bengio, Y. & Haffner, P. (1998). Gradient-based learning applied to document recognition. *Proceedings of the IEEE*, 86(11), 2278-2324. doi: 10.1109/5.726791.

Leelaruji, R. & Vanfretti, L. (2012). State-of-the-art in the industrial implementation of protective relay functions, communication mechanism and synchronized phasor capabilities for electric power systems protection. *Renewable and Sustainable Energy Reviews*, 16(7), 4385-4395. doi: https://doi.org/10.1016/j.rser.2012.04.043.

Leung, K. M. et al. (2007). Naive bayesian classifier. *Polytechnic University Department of Computer Science/Finance and Risk Engineering*, 2007, 123–156.

Malathi, V. & Marimuthu, N. (2008). Multi-class Support Vector Machine approach for fault classification in power transmission line. *2008 IEEE International Conference on Sustainable Energy Technologies*, pp. 67-71. doi: 10.1109/ICSET.2008.4746974.

Mitra, S., Mukhopadhyay, R. & Chattopadhyay, P. (2022). PSO driven designing of robust and computation efficient 1D-CNN architecture for transmission line fault detection. *Expert Systems with Applications*, 210, 118178. doi: https://doi.org/10.1016/j.eswa.2022.118178.

Momesso, A. E., Bernardes, W. M. S. & Asada, E. N. (2019). Fuzzy adaptive setting for time-current-voltage based overcurrent relays in distribution systems. *International Journal of Electrical Power Energy Systems*, 108, 135-144. doi: https://doi.org/10.1016/j.ijepes.2018.12.035.

Ngaopitakkul, A. & Bunjongjit, S. (2013). An application of a discrete wavelet transform and a back-propagation neural network algorithm for fault diagnosis on single-circuit transmission line. *International Journal of Systems Science*, 44(9), 1745-1761. doi: 10.1080/00207721.2012.670290.

Noble, W. S. (2006). What is a support vector machine? *Nature biotechnology*, 24(12), 1565–1567.

O'Shea, K. & Nash, R. (2015). An Introduction to Convolutional Neural Networks. *CoRR*, abs/1511.08458. Retrieved from: http://arxiv.org/abs/1511.08458.

Papaspiliotopoulos, V. A., Korres, G. N., Kleftakis, V. A. & Hatziargyriou, N. D. (2017). Hardware-In-the-Loop Design and Optimal Setting of Adaptive Protection Schemes for Distribution Systems With Distributed Generation. *IEEE Transactions on Power Delivery*, 32(1), 393-400. doi: 10.1109/TPWRD.2015.2509784.

Rai, P., Londhe, N. D. & Raj, R. (2021). Fault classification in power system distribution network integrated with distributed generators using CNN. *Electric Power Systems Research*, 192, 106914. doi: https://doi.org/10.1016/j.epsr.2020.106914.

Ramesh Babu, N. & Jagan Mohan, B. (2017). Fault classification in power systems using EMD and SVM. *Ain Shams Engineering Journal*, 8(2), 103-111. doi: https://doi.org/10.1016/j.asej.2015.08.005.

Ramli, S. P., Mokhlis, H., Wong, W. R., Muhammad, M. A. & Mansor, N. N. (2022). Optimal coordination of directional overcurrent relay based on combination of Firefly Algorithm and Linear Programming. *Ain Shams Engineering Journal*, 13(6), 101777. doi: https://doi.org/10.1016/j.asej.2022.101777.

Ray, P. & Mishra, D. P. (2016). Support vector machine based fault classification and location of a long transmission line. *Engineering Science and Technology, an International Journal*, 19(3), 1368-1380. doi: https://doi.org/10.1016/j.jestch.2016.04.001.

Razavi, F., Abyaneh, H. A., Al-Dabbagh, M., Mohammadi, R. & Torkaman, H. (2008). A new comprehensive genetic algorithm method for optimal overcurrent relays coordination. *Electric Power Systems Research*, 78(4), 713-720. doi: https://doi.org/10.1016/j.epsr.2007.05.013.

Sampaio, F. C., Tofoli, F. L., Melo, L. S., Barroso, G. C., Sampaio, R. F. & Leão, R. P. S. (2022). Adaptive fuzzy directional bat algorithm for the optimal coordination of protection systems based on directional overcurrent relays. *Electric Power Systems Research*, 211, 108619. doi: https://doi.org/10.1016/j.epsr.2022.108619.

Sharaf, H. M., Zeineldin, H., Ibrahim, D. K. & EL-Zahab, E. E.-D. A. (2015). A proposed coordination strategy for meshed distribution systems with DG considering user-defined characteristics of directional inverse time overcurrent relays. *International Journal of Electrical Power Energy Systems*, 65, 49-58. doi: https://doi.org/10.1016/j.ijepes.2014.09.028.

Singh, M., Panigrahi, B. & Abhyankar, A. (2013). Optimal coordination of directional over-current relays using Teaching Learning-Based Optimization (TLBO) algorithm. *International Journal of Electrical Power Energy Systems*, 50, 33-41. doi: https://doi.org/10.1016/j.ijepes.2013.02.011.

Srivastava, N., Hinton, G., Krizhevsky, A., Sutskever, I. & Salakhutdinov, R. (2014). Dropout: a simple way to prevent neural networks from overfitting. *The journal of machine learning research*, 15(1), 1929–1958.

Svozil, D., Kvasnicka, V. & Pospichal, J. (1997). Introduction to multi-layer feed-forward neural networks. *Chemometrics and Intelligent Laboratory Systems*, 39(1), 43-62. doi: https://doi.org/10.1016/S0169-7439(97)00061-0.

Swathika, O. G., Angalaeswari, S., Krishnan, V. A., Jamuna, K. & Daya, J. F. (2017). Fuzzy Decision and Graph Algorithms Aided Adaptive Protection of Microgrid. *Energy Procedia*, 117, 1078-1084. doi: https://doi.org/10.1016/j.egypro.2017.05.231. "First International Conference on Power Engineering Computing and CONtrol (PECCON-2017) 2nd -4th March .2017." Organized by School of Electrical Engineering, VIT University, Chennai, Tamil Nadu, India.

Sánchez-Reolid, R., López de la Rosa, F., López, M. T. & Fernández-Caballero, A. (2022). One-dimensional convolutional neural networks for low/high arousal classification from electrodermal activity. *Biomedical Signal Processing and Control*, 71, 103203. doi: https://doi.org/10.1016/j.bspc.2021.103203.

Tong, H., Qiu, R. C., Zhang, D., Yang, H., Ding, Q. & Shi, X. (2021). Detection and classification of transmission line transient faults based on graph convolutional neural network. *CSEE Journal of Power and Energy Systems*, 7(3), 456-471. doi: 10.17775/CSEEJPES.2020.04970.

Uthitsunthorn, D., Pao-La-Or, P. & Kulworawanichpong, T. (2011). Optimal overcurrent relay coordination using artificial bees colony algorithm. *The 8th Electrical Engineering/ Electronics, Computer, Telecommunications and Information Technology (ECTI) Association of Thailand - Conference 2011*, pp. 901-904. doi: 10.1109/ECTICON.2011.5947986.

Vasconcelos, L. H. P., Almeida, A. R., dos Santos, B. F., Melo, N. X., Carvalho, J. G. S. & de Oliveira Sobreira, D. (2022). Hybrid optimization algorithm applied to adaptive protection in distribution systems with distributed generation. *Electric Power Systems Research*, 202, 107605. doi: https://doi.org/10.1016/j.epsr.2021.107605.

Wang, Z., Oates, T. et al. (2015). Encoding time series as images for visual inspection and classification using tiled convolutional neural networks. *Workshops at the twenty-ninth AAAI conference on artificial intelligence*, 1.

Wang, Z. & Zhao, P. (2009). Fault location recognition in transmission lines based on Support Vector Machines. *2009 2nd IEEE International Conference on Computer Science and Information Technology*, pp. 401-404. doi: 10.1109/ICCSIT.2009.5234528.

Warford, J. S. (2002). Linked Lists. In Hug, K. (Ed.), *Computing Fundamentals: The Theory and Practice of Software Design with BlackBox Component Builder* (pp. 463–514). Wiesbaden: Vieweg+Teubner Verlag. doi: 10.1007/978-3-322-91603-7_21.

Youssef, O. A. (2009). An optimised fault classification technique based on Support-Vector-Machines. *2009 IEEE/PES Power Systems Conference and Exposition*, pp. 1-8. doi: 10.1109/PSCE.2009.4839949.

Yu, J. J. Q., Hou, Y., Lam, A. Y. S. & Li, V. O. K. (2019). Intelligent Fault Detection Scheme for Microgrids With Wavelet-Based Deep Neural Networks. *IEEE Transactions on Smart Grid*, 10(2), 1694-1703. doi: 10.1109/TSG.2017.2776310.

Zeienldin, H., El-Saadany, E. & Salama, M. (2004). A novel problem formulation for directional overcurrent relay coordination. *2004 Large Engineering Systems Conference on Power Engineering (IEEE Cat. No.04EX819)*, pp. 48-52. doi: 10.1109/LESCPE.2004.1356265.

Zeineldin, H., El-Saadany, E. & Salama, M. (2006). Optimal coordination of overcurrent relays using a modified particle swarm optimization. *Electric Power Systems Research*, 76(11), 988-995. doi: https://doi.org/10.1016/j.epsr.2005.12.001.

Zhang, S., Wang, Y., Liu, M. & Bao, Z. (2018). Data-Based Line Trip Fault Prediction in Power Systems Using LSTM Networks and SVM. *IEEE Access*, 6, 7675-7686. doi: 10.1109/ACCESS.2017.2785763.

Zhang, Z. & Sabuncu, M. R. (2018). Generalized Cross Entropy Loss for Training Deep Neural Networks with Noisy Labels.